IOWA STATE UNIVERSITY
Digital Repository

Retrospective Theses and Dissertations

Iowa State University Capstones, Theses and Dissertations

1-1-1977

Plasma confinement in a spherical multipole with octahedral symmetry

Mark Virgil Kaldenberg
Iowa State University

Follow this and additional works at: https://lib.dr.iastate.edu/rtd

Part of the Engineering Commons

Recommended Citation

Plasma confinement in a spherical multipole

with octahedral symmetry

by

Mark Virgil Kaldenberg

A Thesis Submitted to the

Graduate Faculty in Partial Fulfillment of

The Requirements for the Degree of

MASTER OF SCIENCE

Department: Chemical Engineering
             and Nuclear Engineering
     Major: Nuclear Engineering

Iowa State University
Ames, Iowa

1977

TABLE OF CONTENTS

LIST OF FIGURES

Page

LIST OF TABLES

CHAPTER I. ABSTRACT

The inherent magnetohydrodynamic (MHD) stability of cusp-type plasma confinement systems, and the possibility of favorable charged particle confinement in magnetic or hybrid electromagnetic point cusp systems are the two principal motivations for this work. The scope of this thesis is limited to a particular cusped geometry known as an octahedrally symmetric magnetic well which will hereafter be referred to as Osmac (Octahedrally symmetric magnetic confinement). A detailed description of Osmac geometry will be presented. In addition, a method for calculating the magnetic induction from eight filamentary current loops arranged in the Osmac configuration will be developed. This development includes the necessary position and induction vector component transformations for calculating the total magnetic induction at a point from the superposition of the induction contributions from four current loop-pairs. A derivation of the vector potential and magnetic induction of a filamentary current loop, as well as a computer code (the OMIN code) useful for calculating the magnetic induction for Osmac geometry is included in the appendixes.

CHAPTER II.   INTRODUCTION AND LITERATURE REVIEW

The historical development of controlled thermonuclear fusion is replete with a number of unsuccessful confinement schemes in which plasma instabilities greatly diminished the ultimate viability of these approaches (1). Concern over the problem of plasma instabilities forced the development of magnetic confinement concepts in which the configuration of the magnetic field surrounding the plasma effectively dampens perturbations of the confined plasma which lead to instabilities.

In a cusped confinement scheme a plasma is surrounded by magnetic field lines everywhere convex to the trapped plasma. Thus, the center of curvature of the field lines for cusped confinement is nowhere enclosed by the confined plasma (2). A useful energy principle for the study of plasma stability states that the system composed of a plasma and confining magnetic field will seek a state of minimum potential energy if the system is perturbed (3). A study of equilibrium cusp stability after a perturbation is applied shows that an over-all increase in the potential energy of the system will develop (3, 4). Thus, by the energy principle, a cusped confinement system must return to its initial equilibrium state, the state of lowest potential energy available to the system.

Many confinement concepts have been advanced which take advantage of the stability of cusped magnetic fields. This

thesis is a continuation of research into a particular cusped confinement scheme known as an octahedrally symmetric magnetic well (Osmac). Early investigations into the Osmac concept of plasma confinement by Chiu (5), and Valfells et al. (6) indicated that the Osmac concept has a high degree of three dimensional symmetry combined with the stabilizing features of cusped geometries. Osmac is one of a class of confinement geometries in which the magnetic field forms a magnetic well. These magnetic well configurations are often referred to as minimum-B devices since the magnetic induction has a minimum field strength at the center of the device. Minimum-B devices can be divided into two subclassifications, those devices which are adiabatic at $|\vec{B}|_{minimum}$ and those that are not. The correct classification is determined by the following two criteria:

$$|\vec{B}|_{min} > 0, \text{ adiabatic} \tag{a}$$

$$|\vec{B}|_{min} = 0, \text{ nonadiabatic} \tag{b}$$

For the Osmac conductor configuration the magnetic field is zero at the center and increases radially in all directions. Under such an "absolute" minimum-B condition the first abiabatic invariant, $\mu = mv_{\perp}^2/2eB$, of a charged particle rotating about its guiding center is not preserved near the center of the well.

Adiabatic magnetic wells

The design of adiabatic magnetic wells, not necessarily of cusped geometry, is predicated on the expectation that any adiabatic perturbation which causes particles to move away from the minimum-B region will be suppressed by preservation of the first and second adiabatic invariants. If the first invariant is preserved then the translational kinetic energy of the perturbed particle is lost by increasing the gyration energy of the particle. If the second adiabatic invariant

$$J = \int_a^b v_{||} ds$$

is also preserved then the perturbation energy is completely exhausted by increasing $v_\perp$ and $v_{||}$, resulting in a stable particle oscillation between regions of maximum field strength (3). Typical examples of adiabatic magnetic wells are cusp stabilized mirrors (7)—the Baseball and Yin-Yang coil devices.

Nonadiabatic magnetic wells

<u>Cusps</u>   Early theoretical work on cusped magnetic fields was initiated by Berkowitz et al. (8). Basic cusp configurations are shown in Fig. 2.1. For dense, high-β plasmas a field free region exists within the cusp plasma. Particles in this region move in straight lines, i.e., they have an infinite gyroradius. At the plasma boundary a charged particle is returned to the plasma by interaction

(a)

(b)
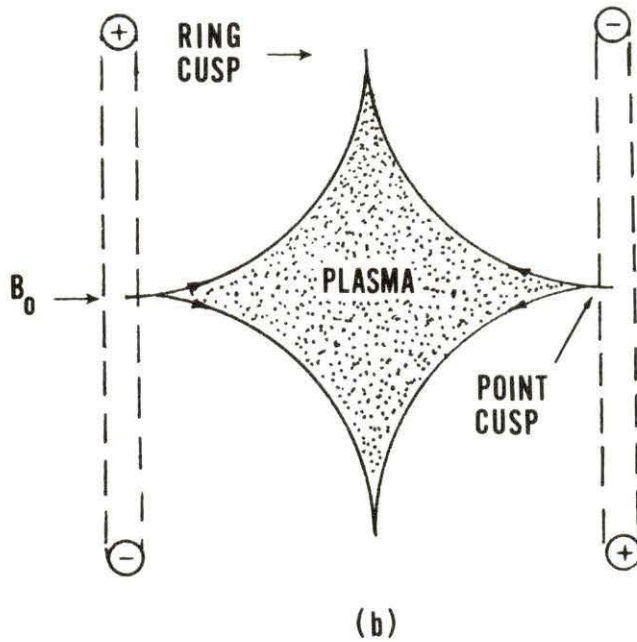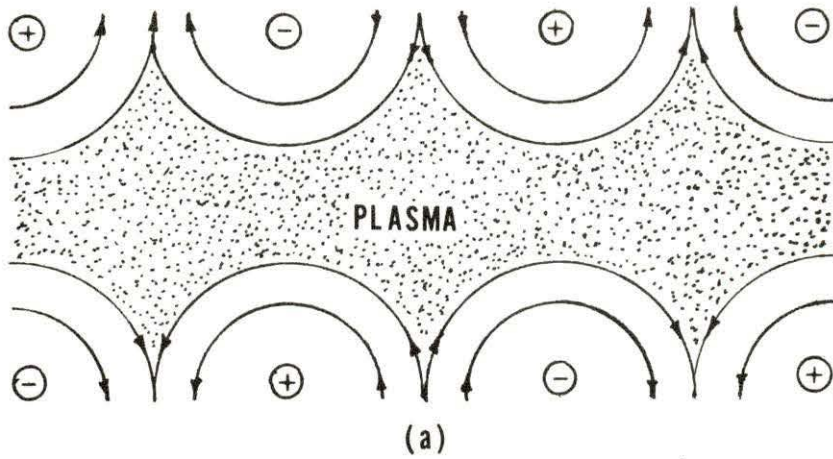
Fig. 2.1.   Two basic cusp confinement configurations
   (a) A picket fence formed from a series of line
       cusps
   (b) A spindle cusp

with the magnetic field. For a sharply defined ($\beta = 1$)
boundary, or "free boundary," the charged particle is bounced
out of the cusp in a near billiard ball reflection (Fig. 2.2a).
For $\beta \lesssim 1$ the plasma is surrounded by a sheath of finite
thickness in which particles follow a cycloidal path back
into the plasma (Fig. 2.2b).

Cusp losses   Cusp systems have the characteristic of
being leaky in the region of the cusps. For low-β plasma,
or plasma away from the minimum-B region, charged particles
stream out adiabatically along the field lines at the cusp.
For $\beta \lesssim 1$ particles stream out of the cusp if r_L, the charged
particle Larmor radius, is too small to turn the particles
back into the field free region. An extensive review of cusp
losses is contained in a review of cusp containment by
Spalding (2). Since cusp containment is nonadiabatic theo-
retical approaches to cusp losses utilize well defined con-
tainment models in which the half-width of the particle loss
hole is to be determined. These loss models assume a high-β
nonadiabatic region away from the cusp which supplies isotropic
plasma to the cusps. The plasma is assumed to be collision-
less. Particle losses through cusps, either the ring or point
cusps of the spindle cusp, are calculated assuming the
mechanism of simple effusion through the loss hole. For a
point cusp

IDEAL PLASMA
BOUNDARY

(a) $\beta = 1$

(b) $\beta < 1$
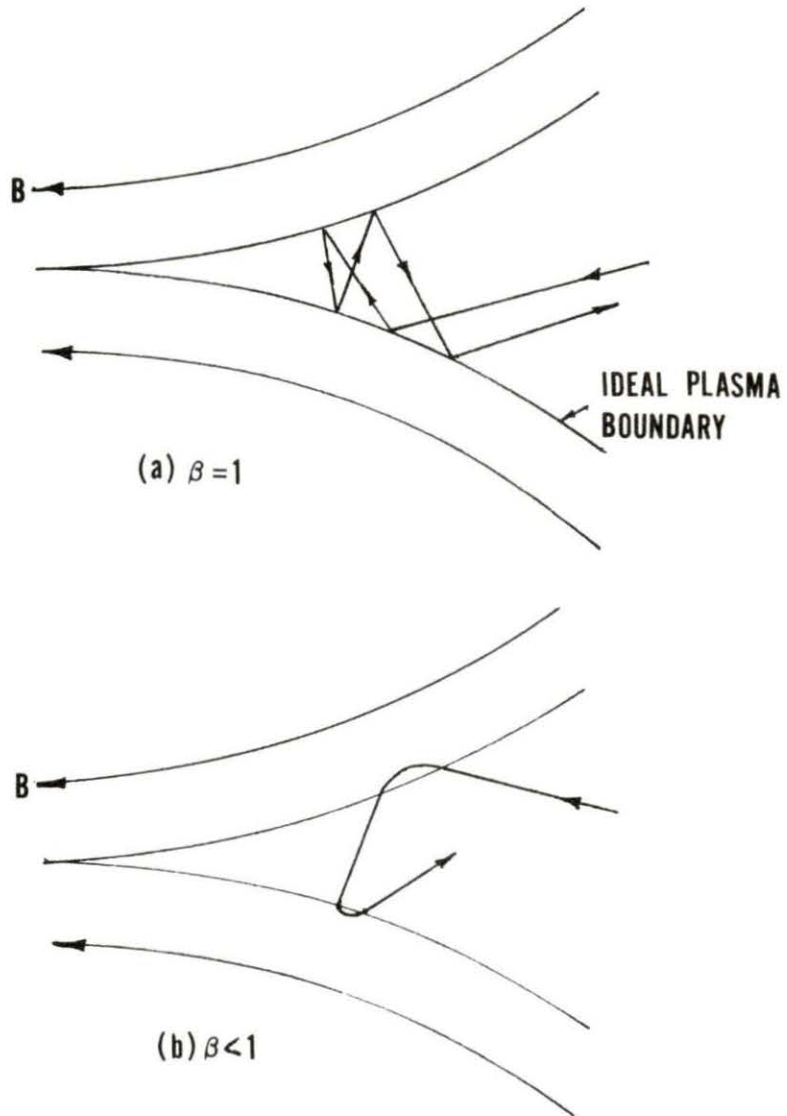
Fig. 2.2. Particle reflection in a two-dimensional cusp (8)

$$\frac{dN}{dt} = \frac{1}{4} \, nv \cdot \pi r_p^2 \qquad (2-1)$$

where

$$v = \sqrt{8kT_i / \pi m_i} \qquad (2-2)$$

is the mean ion thermal speed, n is the ion density, and r_p is the half-width (or radius) of the hole at the point cusp.

In his review of cusp confinement Spalding (2) indicates theoretical and experimental results of cusp losses for two approaches to the formation of free boundary plasma equilibria:

1) Injection of plasma from a field free region into a quasistatic cusp confinement field.

2) Plasma is compressed by a rapidly rising confining cusp field.

Stability experiments confirm the theoretical expectation that cusp confinement is MHD stable.

From these experiments (performed primarily on cusped theta-pinches) the ring and point cusp loss hole half-width was found to be on the order of r_i for $\beta \sim 1$ plasmas. More recent experiments by Kitsunezaki et al. (9) places r_p at some value less than r_i for a laser exploded deuterium pellet in a spindle cusp. Hershkowitz et al. (10) found r_p to be on the order of $2\sqrt{r_i r_e}$, the hybrid gyroradius, for a low-β picket fence line cusp. These results are tabulated in Table 2.1.

Table 2.1.   Experimental determination of r_p for a point cusp

r_p	Method of plasma formation
$\approx r_i$	Plasma injection into cusp field or compression by rising cusp field. $\beta \approx 1.$[a]
$< r_i$	Laser explosion of deuterium ice pellet in spindle cusp. $\beta \approx 1.$[b]
$\approx \sqrt{r_i r_e}$	Low β ($\beta \ll 1$) discharge behind a cusp picket fence. Given r_p is one-half the line cusp half-hole width.[c]

[a]Spalding (2).

[b]Kitsunezaki et al. (9).

[c]Hershkowitz et al. (10).

The octahedrally symmetric magnetic well (Osmac)   The
Osmac concept was initially developed by Valfells et al. (6) and
Chiu (5) to take advantage of the high stability of cusps and
potentially favorable cusp losses. A concept similar to, but
somewhat different from Osmac, employing higher order poly-
hedral symmetry was developed independently by Sadowski (11,
12). The octahedral geometry of the Osmac concept is repre-
sentative of the simplest mode of magnetic wells (or minimum-B
traps) discussed by Sadowski. The geometry of magnetic wells
of this type, called spherical multipoles by Sadowski, are
based on the increasing order of regular polygons--the
tetrahedron, cube, octahedron, dodecahedron, and icosahedron.

Magnetic wells are established by arranging dipoles or current loops on a sphere circumscribing a particular polygon in a manner consistent with the polygonal geometry. For example, dipoles placed at the verticies and concentrically with normals to the geometric center of the faces of a tetrahedron inscribed in a sphere, or at the corners of a cube inscribed in a sphere, or concentric to normals which pass through the centers of the faces of an octahedron all form equivalent magnetic wells.

Sadowski does not extensively treat lower order polygons, concentrating instead on equivalent dodecahedral and icosahedral symmetries. Sadowski also considers only small radius solenoids generating very high fields at the center of the solenoid. With the Osmac geometry treated in this thesis only large radius and overlapping filamentary current loops are treated.

CHAPTER III. THE GEOMETRY OF OSMAC

The geometric description of Osmac is based on the symmetry of an octahedron. It utilizes a principal rectangular coordinate system with axes which intersect the vertices of an octahedron, and four secondary rectangular coordinate systems for each pair of parallel current loops. The symmetry axis of each loop-pair is normal to two parallel faces of an octahedron, and penetrates each triangular face at its geometric center.

The symmetry axis of each loop-pair forms the z-axis of four right-handed rectangular coordinate systems. These positive z-axes are shown in Fig. 3.1. The fifth coordinate system, the principal axes (labeled x_0, y_0, z_0 in Fig. 3.1), define the coordinates to which the magnetic induction contributed by each of the four loop-pairs is transformed and then added. This octahedral geometric description departs from Chiu's (5) tetrahedral description by the addition of a fifth set of axes, the principal set, which is independent from any loop-pair coordinate systems. In Chiu's analysis of the magnetic induction, based on the geometry of the tetrahedron, one of four loop-pair symmetry axes is used as the z-axis of the principal coordinate system. Thus, only three rotation matrices are needed to transform position and induction vector components to and from the remaining three coordinate systems. These rotation matrices allow the magnetic
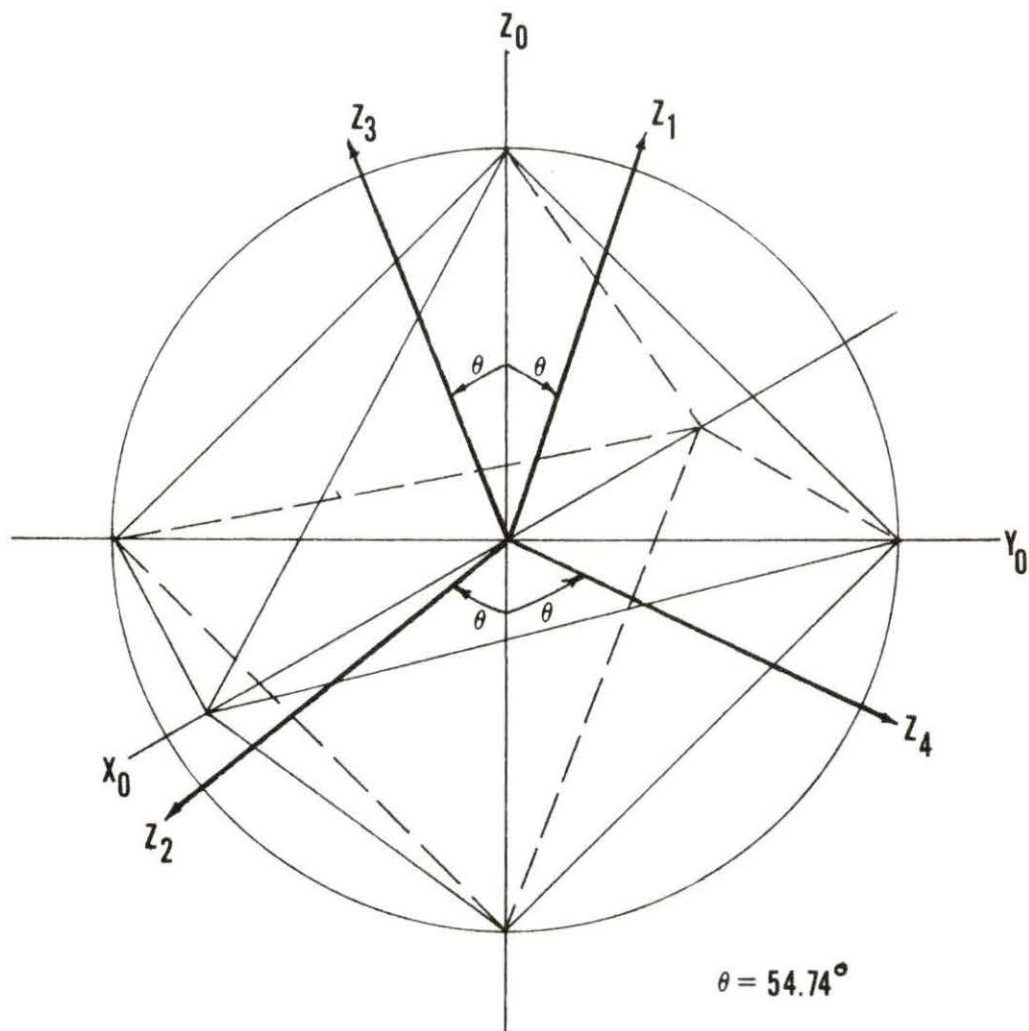
Fig. 3.1. Orientation of the positive z_k-axes with the
principal axes

induction vector components contributed by each loop-pair at a point in the principal system to be transformed to corresponding components in the principal system. The total magnetic induction, contributed to by all four loop-pairs, is simply the superposition of the magnetic inductions contributed by each loop-pair.

With the present analysis the spatial relationship between the current loops is obviously unchanged by the addition of a fifth set of axes. By defining a fifth coordinate system which is independent of each of the loop-pair coordinate systems greater clarity in visualizing the induction field of the magnetic well is achieved. The magnetic induction vector of each loop-pair is now transformed to this loop independent coordinate system. The superposition of the contributions to the total magnetic induction from all four loop-pairs requires four vector transformations. In the notation that follows the subscript zero refers to points or vectors in the principal coordinate system while the subscripts one, two, three, and four refer to the four loop-pair coordinate systems. Table 3.1 shows how the loop-pair coordinate systems are numbered based on the octant in which the positive z-axis of each loop-pair system is located with respect to the principal axes.

Table 3.1. Location of the positive z-axes with respect to
            the principal coordinate system

Positive z-axis number	Octant of the principal axes
1	I
2	III
3	VI
4	VIII

The total magnetic induction at a point P_0 in terms of
the contributions of the four pairs of current loops can be
written

$$\vec{B}_0 = R_1^{-1}\vec{B}_1 + R_2^{-1}\vec{B}_2 + R_3^{-1}\vec{B}_3 + R_4^{-1}\vec{B}_4 \qquad (3-1)$$

$$= \vec{B}_{10} + \vec{B}_{20} + \vec{B}_{30} + \vec{B}_{40} \qquad (3-2)$$

$$= \sum_{k=1}^{4} R_k^{-1}\vec{B}_k \qquad (3-3)$$

where the R_k^{-1}'s are orthogonal 3 x 3 matrices which transform
the components of the four $\vec{B}_k$ induction vectors of each coil
pair to the corresponding components in the principal coordi-
nate system. The total induction vector in component form is
just

$$B_{0i} = \sum_{k=1}^{4} \sum_{j=1}^{3} a_{ijk}b_{jk} , \quad i = 1, 2, 3. \qquad (3-4)$$

The subscript k indicates in which loop-pair coordinate system the vector b_{jk}, j = 1, 2, 3 is located and which 3 x 3 matrix composed of a_{ij} components transforms the vector components b_{jk} to the principal coordinate system. The a_{ijk} elements form a 3 x 3 x 4 array in which the a_{ijk}, k = 1, 2, 3, 4 elements are the direction cosines of a rotation of the principle axes to form the four loop-pair coordinate systems.

The induction vector at a point, resulting from the superposition of induction vectors contributed by the four loop-pairs, requires finding both the elements a_{ijk} of the transformation matrices and a suitable vector potential $\vec{A}$ for calculating $\vec{B} (= \nabla \times \vec{A})$ from each loop-pair.

The R_k elements are calculated by knowing that the axes of the loop-pair coordinate systems must satisfy two conditions.

1. The axes of a loop-pair coordinate system are formed by a right-handed, or "proper," rotation of the principal axes. The determinant of the resulting transformation matrix R_k must be +1.

2. The $+z_k$-axis, or symmetry axis of each loop-pair, must make an angle of 54.73561° with the $\pm z_0$-axis depending on the octant in which the +z-axis is located (cf. Fig. 3.1).

The second condition insures the z_k-axis is normal to the face of the octahedron and passes through the geometric center.

Transformation of vector components from principal components $(x,y,z)_0$ to corresponding components in any one of the four loop-pair coordinate systems is equivalent to finding new components of the vector after an orthogonal rotation of the principal axes in three dimensions. Under such a rotation the magnitude of a vector remains unchanged. The four required rotations of the principal axes can be accomplished by the product of two plane rotations.

1. Rotation of the x_0, y_0 plane counterclockwise around the z_0-axis to fix the new x_k, $k = 1, 2, 3, 4$ axes.

2. Rotation of the y_0, z_0 plane counterclockwise around the x_k-axes to establish the position of the z_k-axes under condition 2 above.

The product of the matrices which mathematically accomplish these rotations can be written

$$R_k = M_k N_k \, , \qquad (3-5)$$

where

$$M_k = \begin{bmatrix} \cos\phi_k & -\sin\phi_k & 0 \\ \sin\phi_k & \cos\phi_k & 0 \\ 0 & 0 & 1 \end{bmatrix} \qquad (3-6)$$

and ϕ_k is the angle of rotation of the x_0, y_0 plane counter-clockwise around the z_0 axis.

$$N_k = \begin{bmatrix} 1 & 0 & 0 \\ 0 & \cos\theta_k & -\sin\theta_k \\ 0 & \sin\theta_k & \cos\theta_k \end{bmatrix} \qquad (3\text{-}7)$$

where θ_k is the angle of rotation of the z_0, y_0 plane counter-clockwise around the x_k-axis.

Taking the product,

$$R_k = M_k N_k = \begin{bmatrix} \cos\theta_k & \sin\phi_k & 0 \\ -\sin\phi_k \theta_k & \cos\phi_k \cos\theta_k & \sin\theta_k \\ \sin\phi_k \sin\theta_k & -\cos\phi_k \sin\theta_k & \cos\theta_k \end{bmatrix} \cdot \qquad (3\text{-}8)$$

The ϕ_k and θ_k for each rotation is tabulated below.

Table 3.2.   Rotation angles for each loop-pair rotation

R_k	θ_k°	ϕ_k°
1	54.73561	135
2	234.73561	225
3	54.73561	315
4	234.73561	45

By substitution of ϕ_k and θ_k from Table 3.2 into Eq. 3-8 the R_k can be explicitly evaluated.

$$R_1 = \begin{bmatrix} -0.707107 & 0.707107 & 0.000000 \\ -0.408248 & -0.408248 & 0.816497 \\ 0.577350 & 0.577350 & 0.577350 \end{bmatrix} \qquad (3\text{-}9)$$

$$R_2 = \begin{bmatrix} -0.707107 & -0.707107 & 0.000000 \\ -0.408248 & 0.408248 & -0.816497 \\ 0.577350 & 0.577350 & 0.577350 \end{bmatrix} \qquad (3\text{-}10)$$

$$R_3 = \begin{bmatrix} 0.707107 & -0.707107 & 0.000000 \\ 0.408248 & 0.408248 & 0.816497 \\ -0.577350 & -0.577350 & 0.577350 \end{bmatrix} \qquad (3\text{-}11)$$

$$R_4 = \begin{bmatrix} 0.707107 & 0.707107 & 0.000000 \\ 0.408248 & -0.408248 & -0.816497 \\ -0.577350 & 0.577350 & -0.577350 \end{bmatrix} \qquad (3\text{-}12)$$

Since $\det|R_k| = +1$, $k = 1, 2, 3, 4$ the four rotations of the principal coordinate axes are right-handed. The orthogonality of the R_k implies the equivalence of the transpose and inverse of R_k

$$R_k^{-1} = R_k^T \qquad (3\text{-}13)$$

In order to find the components of a vector in any one of the four loop-pair coordinate systems in term of its principal coordinates requires multiplying that vector by the correct inverse transformation matrix R_k^{-1}, so that

$$\vec{B}_{k0} = R_k^{-1}\vec{B}_k = R_k^T\vec{B}_k \qquad (3\text{-}14)$$

where the components of $\vec{B}_k$ are known.

The procedure for finding the magnetostatic induction at any point in the Osmac geometry is now apparent.

1. The $(x,y,z)_0$ ordered triplet specifying the position vector of a point P_0 in the principal coordinate system is determined.

2. The $(x,y,z)_0$ components are transformed into the $(x,y,z)_k$ components of each loop-pair coordinate system by use of the proper R_k transformation matrix.

3. The vector components of the magnetic induction vector $\vec{B}_k$ at the point specified in step 1 are determined.

4. The components of $\vec{B}_k$ for each loop-pair are transformed by R_k^{-1} into the corresponding components in the principal coordinate system.

5. The total magnetic induction at P_0 is the sum of the four inductions calculated for each loop-pair,

$$\vec{B}_0 = \vec{B}_{01} + \vec{B}_{02} + \vec{B}_{03} + \vec{B}_{04} = \sum_{k=1}^{4} \vec{B}_{0k}$$

CHAPTER IV. THE MAGNETIC INDUCTION OF A CONCENTRIC
PAIR OF CIRCULAR CURRENT LOOPS

The calculation of the induction for a pair of axisym-
metric current loops requires an expression for $\vec{B}_k$. To
calculate the induction at a point resulting from Osmac
geometry the current loops are assumed to be infinitly thin
(filamentary). The potential of an arbitrary closed loop at
a point P is

$$\vec{A}_p = \frac{\mu_o I}{4\pi} \cdot \oint \frac{\vec{ds}}{|\vec{R}|} \tag{4-1}$$

where $|\vec{R}|$ is the distance from loop element $\vec{ds}$ to the point
P. The method for finding $\vec{A}_p$ for a circular loop in a form
useful for computation can be found in most introductory
texts on electromagnetism (13).

As shown in Fig. 4.1,

$$\vec{a} = a(\cos\phi\hat{i} + \sin\phi\hat{j}). \tag{4-2}$$

A differential element of the circular loop can be written

$$\vec{ds} = a(-\sin\phi\hat{i} + \cos\phi\hat{j})d\phi \tag{4-3}$$

The vector potential can be rewritten as (cf. Fig. 4.1)

$$\vec{A}_p = \frac{\mu_o I a}{4\pi} \cdot \int_0^{2\pi} \frac{(-\sin\phi\hat{i} + \cos\phi\hat{j})d\phi}{(\rho^2 + a^2 + z^2 - 2ap\cos(\phi-\xi))^{\frac{1}{2}}} \tag{4-4}$$

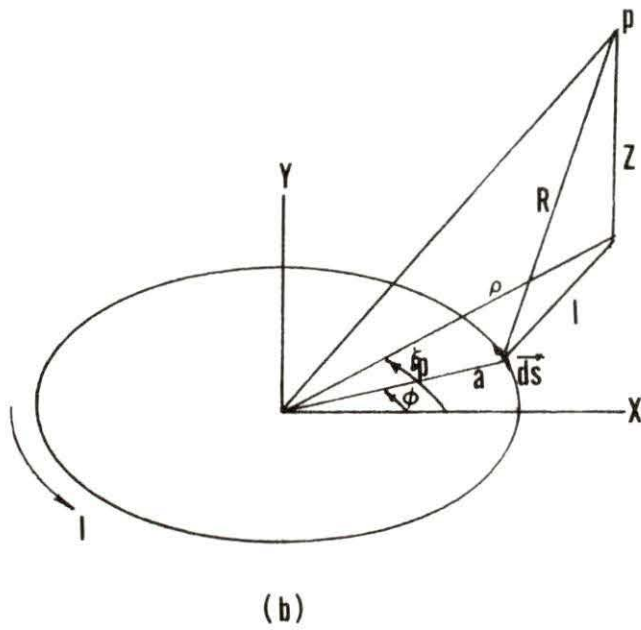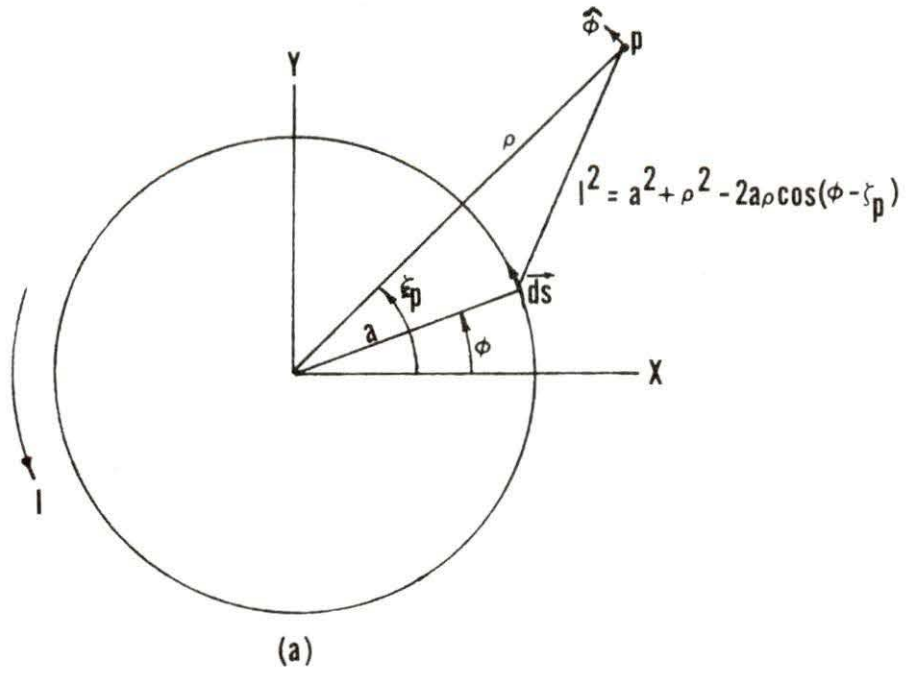$$l^2 = a^2 + \rho^2 - 2a\rho\cos(\phi - \zeta_p)$$

(a)

(b)

Fig. 4.1. Coordinates and directions for the evaluation of
the vector potential of a circular current loop

Since $\vec{A}_p$ is ϕ symmetric $\vec{A}_p$ at $\xi_p = 0$ can be generalized for any ξ_p.

Let

$$\vec{A}_p = \vec{A}_0(\xi = 0) \qquad (4-5)$$

$$k^2 = \frac{4a\rho}{[(a + \rho)^2 + z^2]} \qquad (4-6)$$

$$|\vec{R}| = [(a + \rho)^2 + z^2]^{\frac{1}{2}}(1 - k^2 \sin^2\alpha)^{\frac{1}{2}} \qquad (4-7)$$

where

$$\sin^2\alpha = \frac{1}{2}(1 + \cos\phi) \qquad (4-8)$$

Eq. 4-4 can be written (cf. Appendix A),

$$\vec{A}_0 = \frac{\mu_0 I}{4\pi} \left(\frac{a}{\rho}\right)^{\frac{1}{2}} \left\{ \hat{i} \int_{-\frac{\pi}{2}}^{\frac{\pi}{2}} \frac{2\sin\alpha\cos\alpha\, d\alpha}{\sqrt{1-k^2\sin^2\alpha}} - \hat{j} \int_{-\frac{\pi}{2}}^{\frac{\pi}{2}} \frac{(2\sin^2\alpha - 1)\, d\alpha}{\sqrt{1-k^2\sin^2\alpha}} \right\} \qquad (4-9)$$

The integral coefficient of $\hat{i}$ is zero. The coefficient of $\hat{j}$ can be rewritten in the form,

$$\vec{A}_p = \frac{\mu_0 I}{\pi k} \left(\frac{a}{\rho}\right)^{\frac{1}{2}} \left[\left(1 - \frac{k^2}{2}\right) K(k) - E(k) \right] \hat{\phi} \qquad (4-10)$$

where $\vec{A}_0$ has been generalized to show $\hat{\phi}$ symmetry. $K(k)$ and $E(k)$ are the complete elliptic integrals of the first and second kind respectively, k is the modulus and α is the

amplitude of the elliptic integral.

Taking the curl of $\vec{A}_p$, the magnetic induction at P is

$$\vec{B}_p = \frac{\mu_0 I}{4\pi a^{\frac{1}{2}} \rho^{3/2}} \left\{ -z\left[K(k) - \left[\frac{1 - k^2/2}{1 - k^2} \right] E(k) \right] \hat{\rho} \right.$$
$$\left. + \rho\left[K(k) + \left[\frac{(a + \rho)k^2}{2\rho} - 1 \right] \frac{E(k)}{(1-k^2)} \right] \hat{z} \right\}.$$

$$(4-11)$$

For $\rho = 0$ Eq. 4-11 reduces to the familiar expression

$$\vec{B}_{axis} = \frac{\mu_0 I}{2} \frac{R^2}{(R^2 + z^2)^{3/2}} \hat{z}.$$

$$(4-12)$$

For an axisymmetric pair of current loops the magnetic induction at a point in space is the superposition of the magnetic induction contributed by each current loop (Fig. 4.2). For a pair of current loops, in cylindrical coordinates with both currents in the positive ϕ direction, the magnetic induction has the form resulting from a simple mirror configuration. For currents anti-parallel in the ϕ direction the induction has the form of the familiar spindle cusp configuration. The expression for $\vec{B}_p$ of two parallel, axisymmetric loops satisfying the condition $D = \sqrt{2}a$, where D is the separation distance and a is the radius of each loop, is then

$$\vec{B}(\rho, z) = \vec{B}(\rho, z - \frac{\sqrt{2}}{2} a) \pm \vec{B}(\rho, z + a \frac{\sqrt{2}}{2}).$$
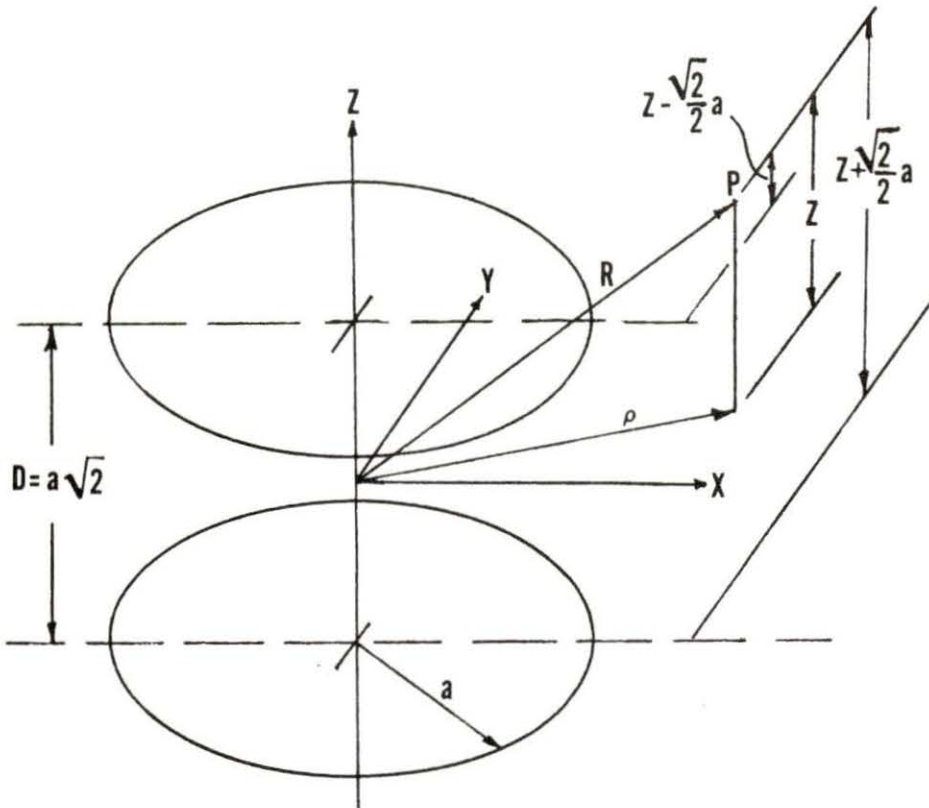
$$(4-13)$$

Fig. 4.2. Orientation of a loop-pair symmetric with the z_k-axis and the location of point P with respect to the origin

CHAPTER V.   RESULTS OF THE OMIN CODE FOR CALCULATING
OSMAC MAGNETIC INDUCTION

Knowledge of the internal magnetic induction from cur-
rent loops arranged in the Osmac configuration on a contain-
ment sphere of radius R_c is useful for determining, at least
qualitatively, the plasma confining properties of the system.
Utilizing Eqs. 3-4 and 4-11 a computer code, called OMIN, was
developed which is capable of calculating the eight loop
magnetic induction for a filamentary current loop approxima-
tion. Loop radii were based on a twelve liter sphere which
will be used for plasma trapping experiments. The sphere
gives a loop radius of 11.596 cm. The magnitude of the loop
current is arbitrary.

An objective of the code calculations was to compare the
"depth" of various simple magnetic well configurations with
parallel loops satisfying the relationship $D_L = \sqrt{2}\ a_L$. The
loop configurations compared were a simple mirror pair, a
cusped pair, Osmac in the cusp mode with loop-pairs having
currents in opposing directions, and Osmac in the mirror mode
with loop-pairs having currents in the same direction (Eq.
4-13).

Fig. 5.1 shows the variation in $|\vec{B}|$ along the symmetry
z-axis, or z_1-axis for Osmac, for the above four configurations.
From Fig. 5.1 it is evident that the Osmac configuration sur-
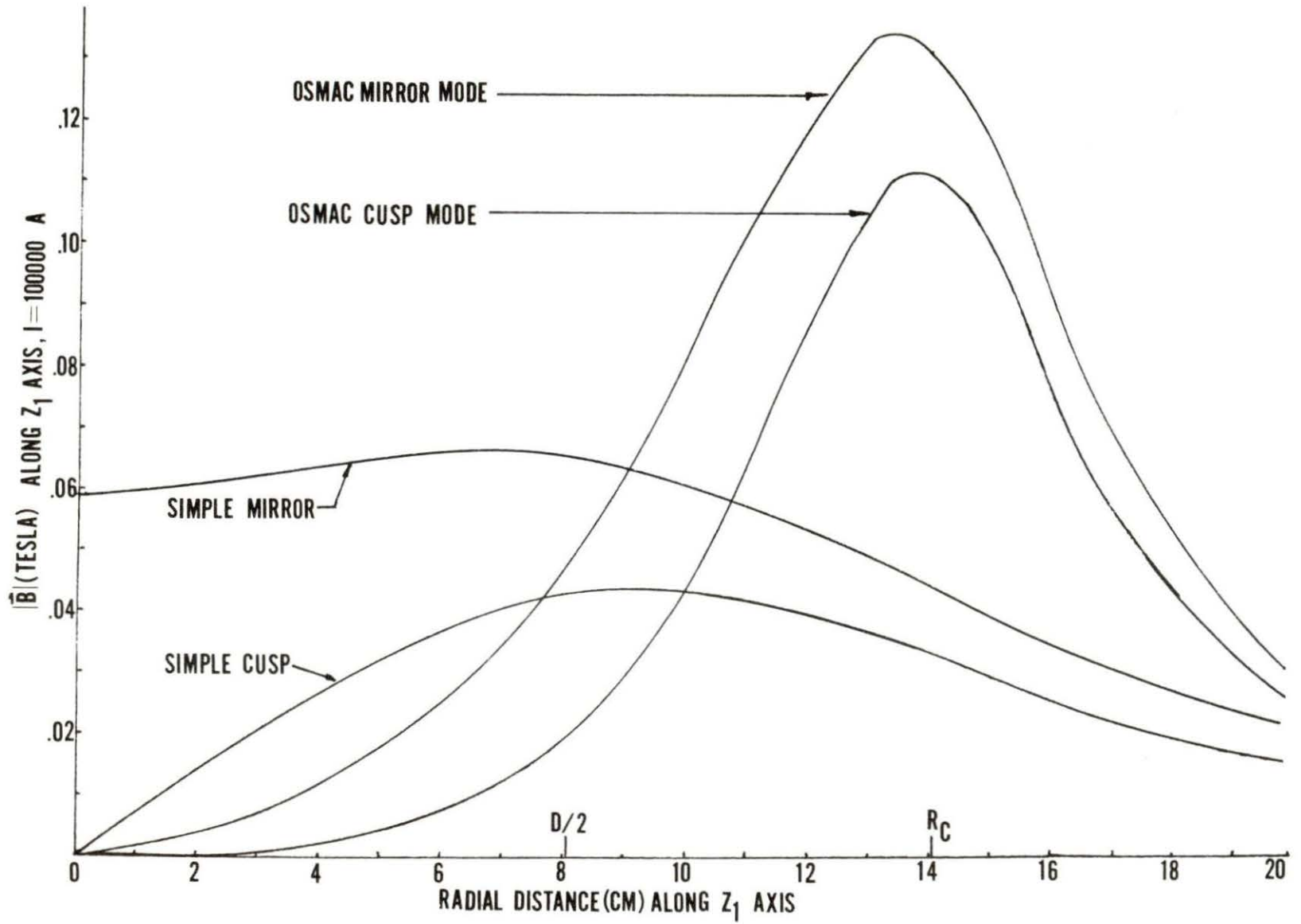passes both the two-loop mirror and cusp configurations in

Fig. 5.1.   The variation of $|\vec{B}|$ as a function of z_1 for four loop configurations

26

peak field strength for identical currents. The location of
the peak for the Osmac conductor configuration is also dis-
placed away from the plane of the current loops toward the
containment surface at R_c.

Fig. 5.2 shows the variation in magnitude of the peak
for Osmac in the mirror mode along the z_k, $k = 1, 2, 3, 4$
axes as a function of current. As expected from Eqs. 4-11
and 4-12 the peak value varies linearly with current in the
filamentary loops. Similar to the two loop cusp configuration
the Osmac loop configuration, in either the mirror or cusp
modes, has zero induction at the geometric center. Since the
magnetic moment of charged particles is not preserved at the
center of the configuration Osmac is a nonadiatatic magnetic
well.

A second objective of the code was to plot magnetic
magnetic isobars, lines of constant magnetic induction $|\vec{B}|$,
in two planes of the principal coordinate system. The loca-
tion of these planes is best described in terms of a set of
spherical coordinates (ρ, θ, ϕ) associated with the principal
rectangular axes as shown in Fig. 5.3.

The two mapping planes selected were the quarter-planes
$P_1(\phi = 45°, \theta = 0° \rightarrow 90°)$ and plane $P_2(\phi = 0° \rightarrow 90°, \theta = 90°)$.
The P_1 plane contains the z_1-axis and should indicate the
presence of a cusp symmetric with the z_1-axis. This cusp
arises from the triangular pattern of conductors axisymmetric
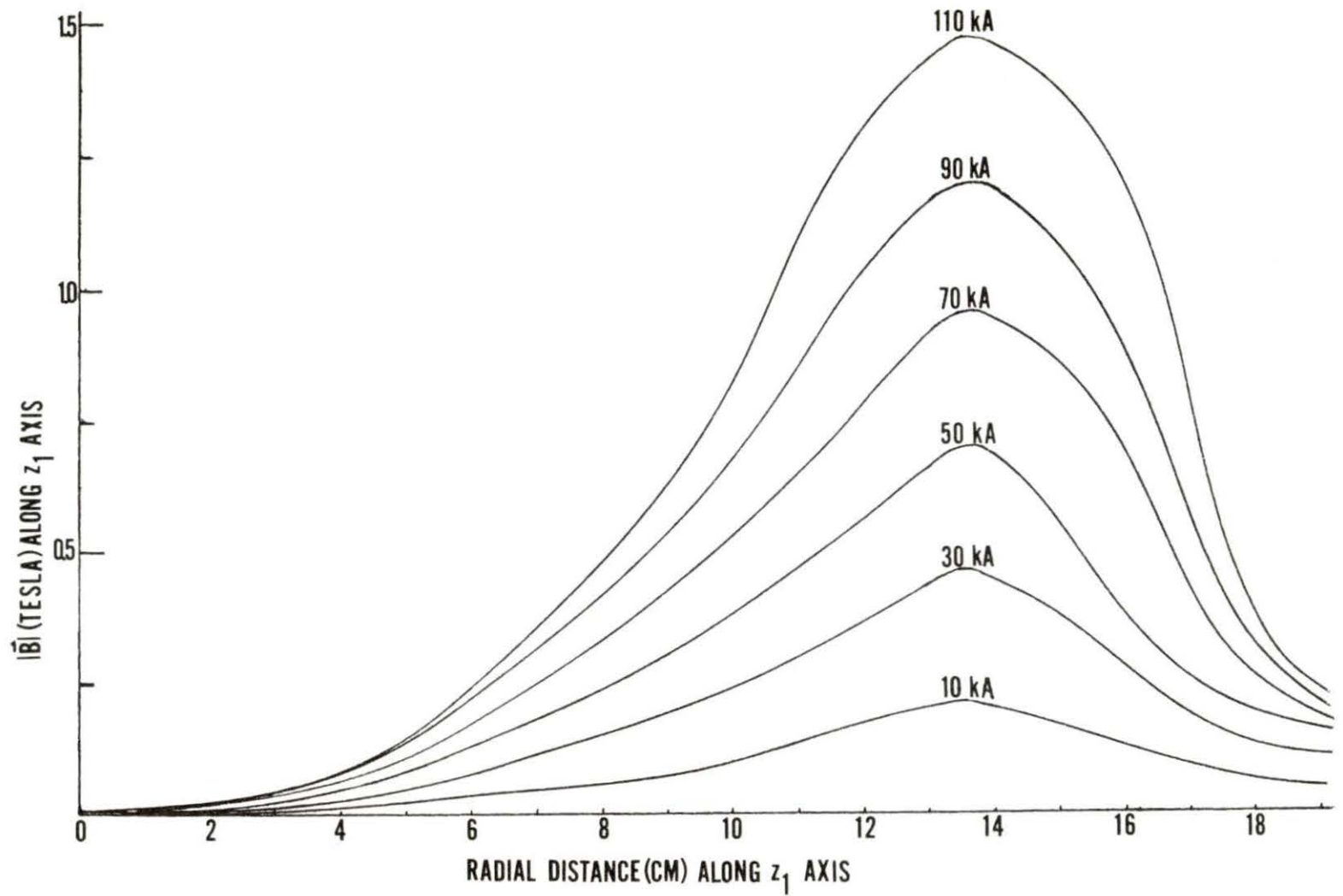
Fig. 5.2. The variation of $|\vec{B}|$ along z_1 as a function of both distance and current
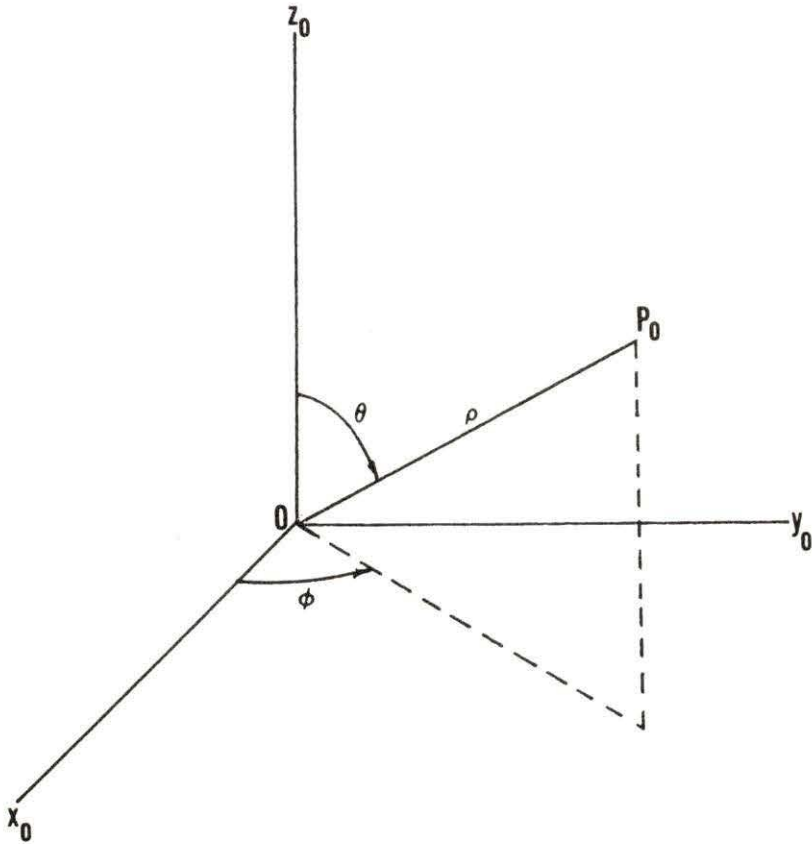
Fig. 5.3. The location of point P_0 with respect to both the cartesian and spherical coordinates of the principal axes

with the z_1-axis as shown in Fig. 5.4. Plane P_2 is one of three quarter-planes which form the sides of the first octant of the principal coordinate system. The symmetry of the Osmac configuration insures that the induction is identical in these three quarter-planes. Iso-$|\vec{B}|$ lines generated by the two modes of Osmac, the cusp and mirror modes, were mapped.

Figure 5.5 shows plane P_1 in the cusp mode. As anticipated a cusp is formed symmetric with the z_1-axis ($\theta = 54.74°$, $\phi = 45°$). A second cusp is formed symmetric with the $\theta = 90°$, $\phi = 45°$ radius. This cusp results from the currents in loops symmetric with the z_1 and z_3 axes (See Fig. 5.9). Plane P_2 in the cusp mode, shown in Fig. 5.6, shows the presence of a cusp at low field strengths which broadens and reverses direction at 0.3 tesla ($I = 100000$ amps). It is not apparent from iso-$|\vec{B}|$ plots if the field line curvature favors stability since the two lines are not necessarily identical. However iso-$|\vec{B}|$ lines do show the location of cusps and the direction in which they point, either toward or away from the center of the Osmac configuration. Cusps which point away from the center can be considered stable for plasma confinement. Hence, for high field strengths, the Osmac configuration in the cusp mode favors stability.

Figure 5.7 shows plane P_1 in the Osmac mirror mode. Favorable although shallow cusping is obtained away from the z_0-axis. The cusp at $\theta = 54.74°$ is evident as well as a cusp
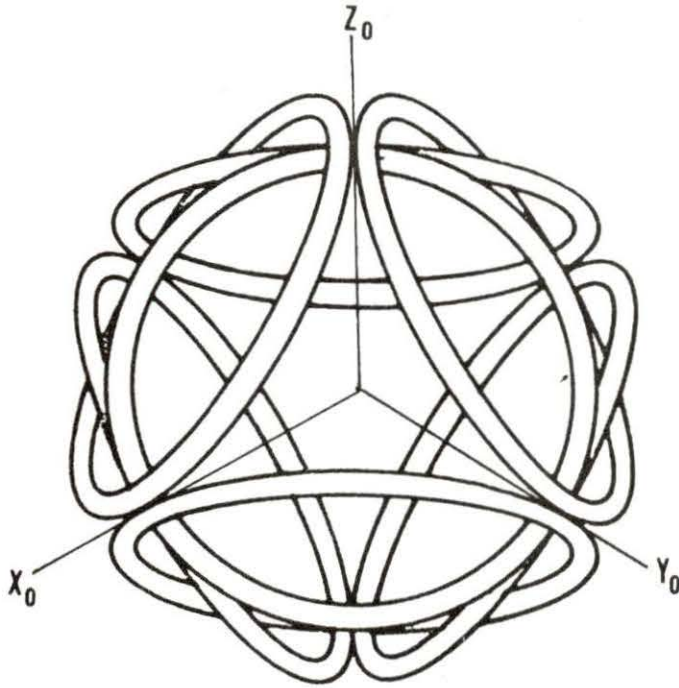
Fig. 5.4.   The spatial arrangement of the eight Osmac current
loops
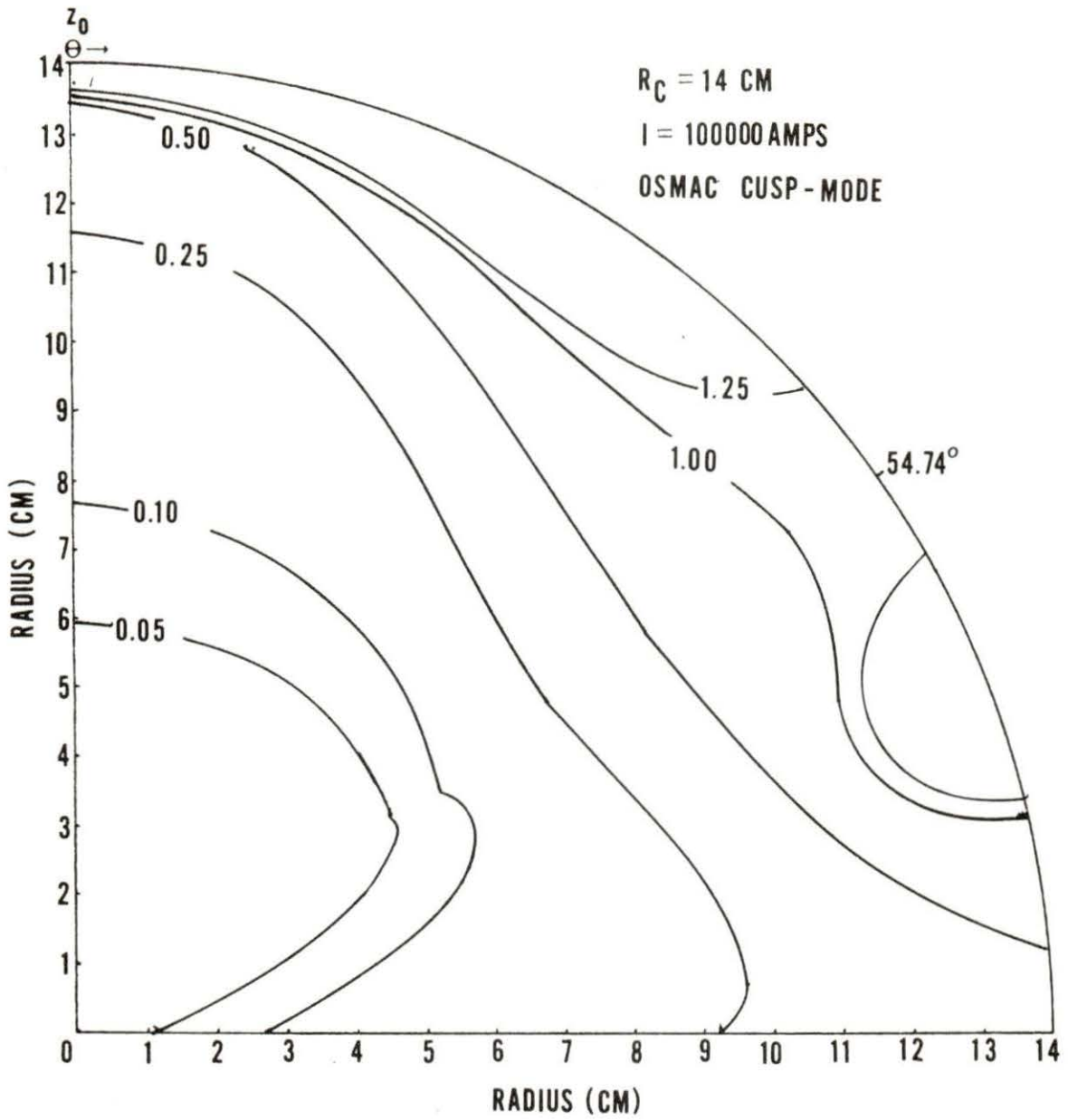
Fig. 5.5.   The P_1 plane in the cusp-mode
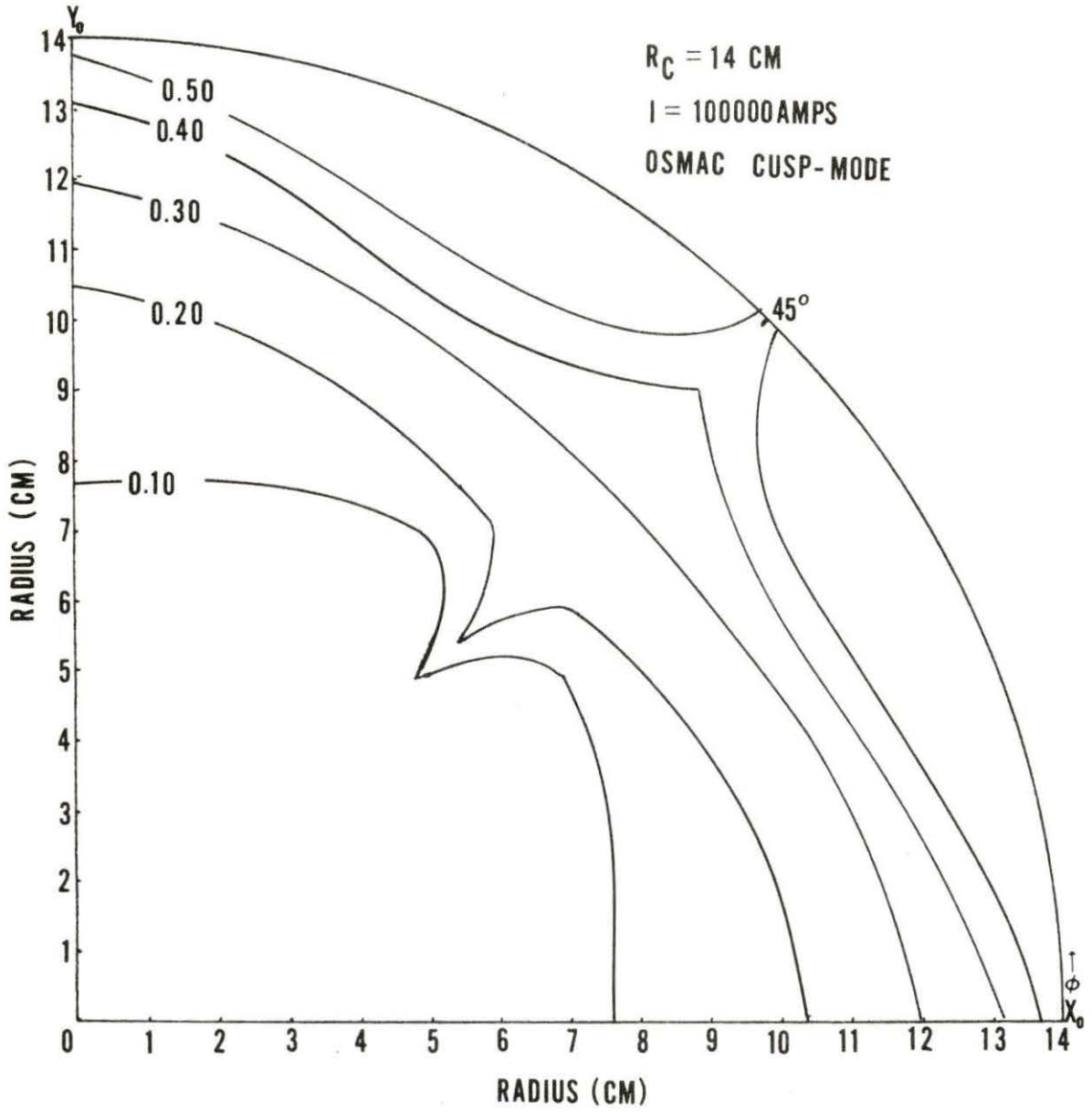
Fig. 5.6.   The P_2 plane in the cusp-mode
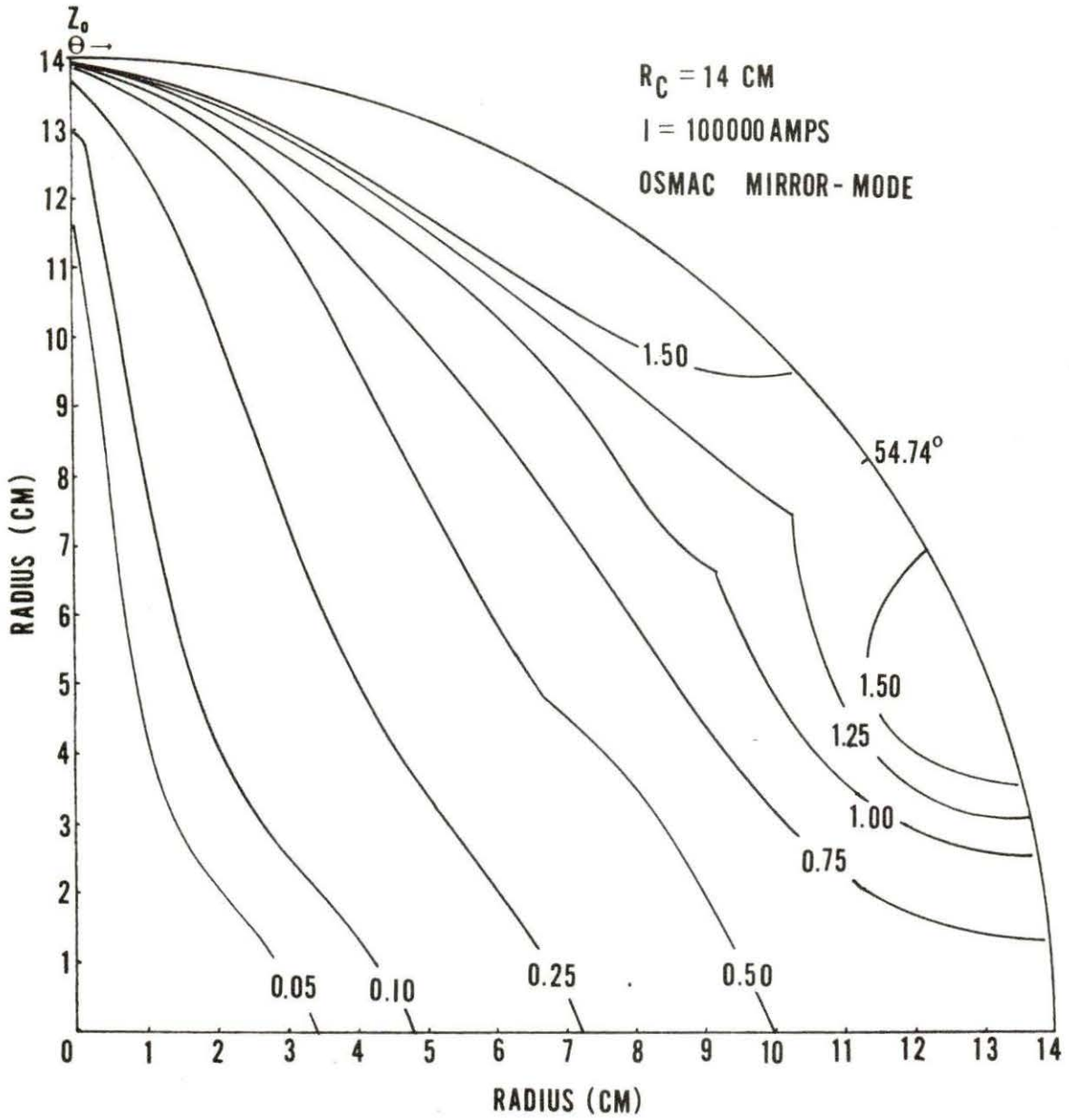
Fig. 5.7.   The P_1 plane in the mirror-mode

at $\theta = 90°$ formed by the z_1 and z_3 axisymmetric loops. Figure 5.8 shows the P_2 plane in the mirror mode. The cusp at $\phi = 45°$ is again evident. Unlike the previous mode this cusp does not change direction away from the center of the Osmac configuration. The direction of the cusps favor stability away from the principal axes. In the P_2 plane the maximum induction is located well inside R_c. This maximum is due to the effect of overlapping current loops as shown in Fig. 5.9.

36
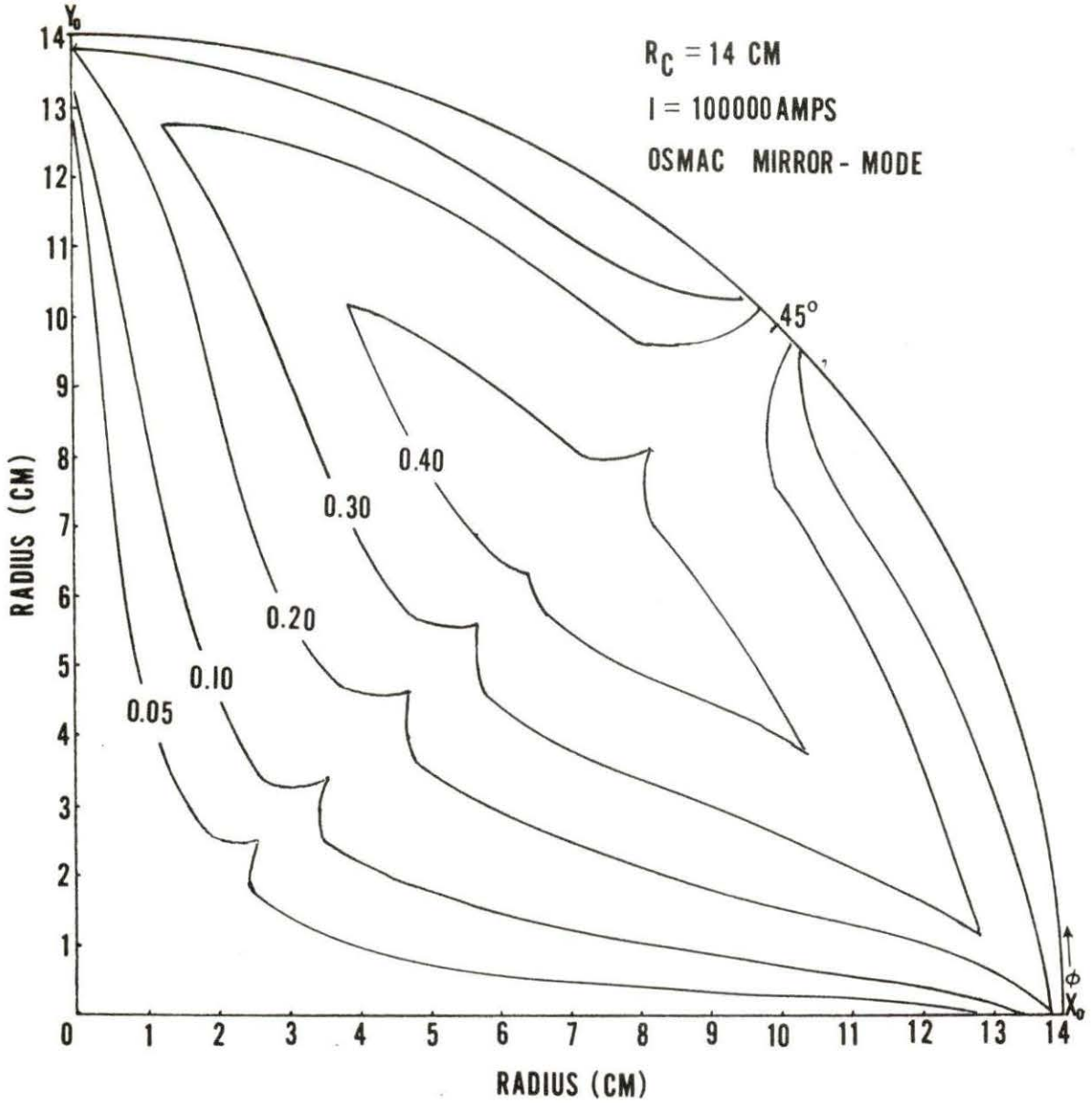
Fig. 5.8. The P$_2$ plane in the mirror-mode
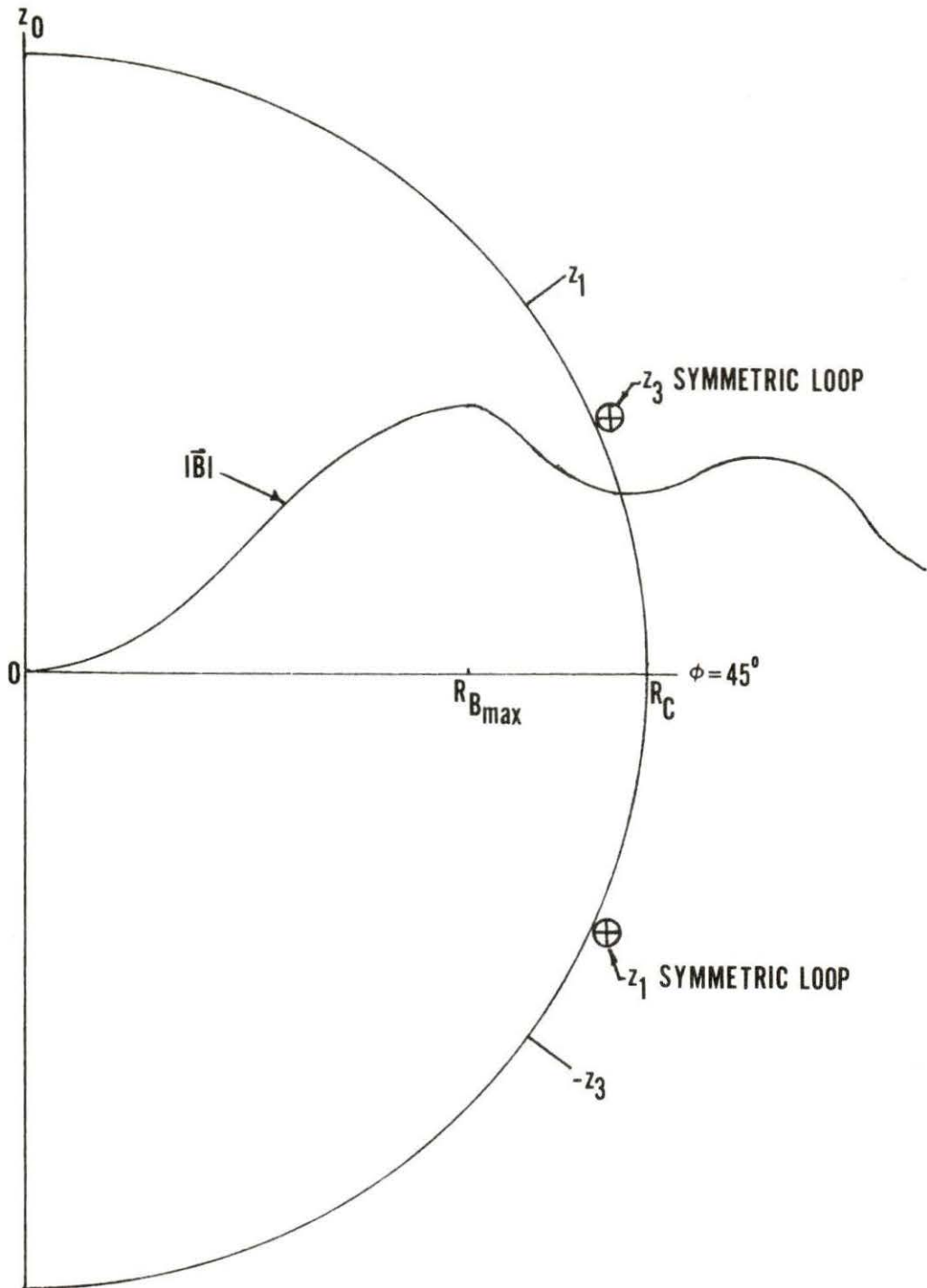
Fig. 5.9. The effect of overlapping current loops on the induction in plane P_2 in the mirror mode

CHAPTER VI.   CONCLUSIONS

Osmac is an "open" cusped confinement system and as such suffers from particle losses characteristic of cusped systems. Using the model of filamentary current loops and the $D_L = \sqrt{2}\ a_L$ constraint on loop-pair separation the Osmac configuration has eight point cusps axisymmetric with the z_k, $k = 1$, 2, 3, 4 axes, as well as twelve line cusps associated with the loop overlap indicated in Figs. 5.4 and 5.9. Methods to eliminate the line cusps will be given in the recommendations for future work. An estimate of cusp losses for eight point cusps with line cusps eliminated can be made using Eq. 2-1 and values of r_p from Table 2.1. We assume the following:

1. Steady state plasma equilibrium
2. $B_0 = 5 \times 10^4$ gauss (a reasonable value with current technology)
3. $T_i = T_e = 10$ keV
4. D-T plasma with $m_i = \dfrac{m_D m_T}{m_D + m_T}$

5. $n = 1 \times 10^{14}$ ions/cm^3

The equation for the Larmar radius of a charged particle is

$$r_\pm = \frac{m_\pm c}{e B_0} \sqrt{\frac{3kT}{m_\pm}} \qquad (6\text{-}1)$$

where $\pm$ denotes the charged particle species, an ion (+) or electron (-).

Using assumptions 1 through 5, Eqs. 2-1, 2-2, and 6-1 charged particle losses through the cusps can be estimated for two cases.

1. $r_p = r_i$

$$v = 1.42 \times 10^8 \text{ cm/sec}$$

$$r_i = 0.388 \text{ cm}$$

$$\frac{dN}{dt} = 8 \times \frac{1}{4} n \, v\pi r_p^2 = 1.34 \times 10^{22} \text{ ions/sec}$$

$$= 2152 \text{ amps.}$$

2. $r_p = \sqrt{r_i r_e}$

$$r_e = 7.54 \times 10^{-3} \text{ cm}$$

$$\frac{dN}{dt} = 6.53 \times 10^{20} \text{ ions/sec}$$

$$= 42 \text{ amps.}$$

If r_p is closer to the geometric mean of the hybrid gyroradius, and recent experiments tend to indicate this is near the correct value of r_p, then cusp losses are reduced ninety-eight percent over losses with $r_p = r_i$. This is a very impressive result. Since the first assumption is a steady plasma equilibrium these loss calculations define the required makeup to maintain constant ion density of the plasma. Injection in the worst case ($r_p = r_i$) requires a makeup on the order of 270 amps per cusp, an impractical amount. For the

best case ($r_p = \sqrt{r_i r_e}$) a makeup injection of 5 to 6 amps per cusp is certainly within the realm of feasibility. Which value on the makeup does pertain will depend on further research into point cusp losses.

Any conclusions about confinement feasibility drawn from these estimates of charged particle losses are also tentative for the following reasons.

1. No mention has been made of other mechanisms of particle particle losses, especially diffusion across the magnetic field.

2. Ion losses are proportional to the steady state equilibrium plasma density. It may ultimately turn out that the steady state density requirement for fusion will entail an impractical makeup current. This point deserves careful attention since Osmac confinement has been suggested as a viable approach to target plasma fusion.

3. No consideration was given to the ion injection energy and the effect ion slowing down would have on the plasma equilibrium. A departure of plasma equilibrium away from a Maxwellian energy distribution may upset the assumption of simple effusion out the cusp.

CHAPTER VII.   RECOMMENDATIONS FOR FUTURE WORK

Recommendations for further studies on the Osmac concept are ultimately geared toward reduction of charged particle losses by reducing the number of cusps generated by the loop configuration. An improvement in the adiabaticity of the con-figuration should also result in improved particle confinement and a well understood loss mechanism.

1. Reducing the number of cusps to eight results when the circular current loops are replaced by either plane triangular or spherical triangular current loops which share common borders. This new Osmac configuration is shown in Fig. 7.1. It should be noted that in the mirror mode adjacent conductor currents are additive. An alternative approach is to replace current loops or triangles with small radius dipoles.

2. Particle losses at the cusps may be reduced by utilizing Osmac geometry as a hybrid electromagnetic trap. This approach entails "stoppering" with electrostatic fields the cusps produced by the magnetostatic field.

3. A study should be undertaken to look into the effect of "stuffing" the system with a mirror field. This approach to improved confinement, utilized by Sadowski (14) in his research on higher order spherical multipoles, removes the field zero at the center of the geometry. The result of stuffing is to preserve the charged particle magnetic moment

(a)

(b)
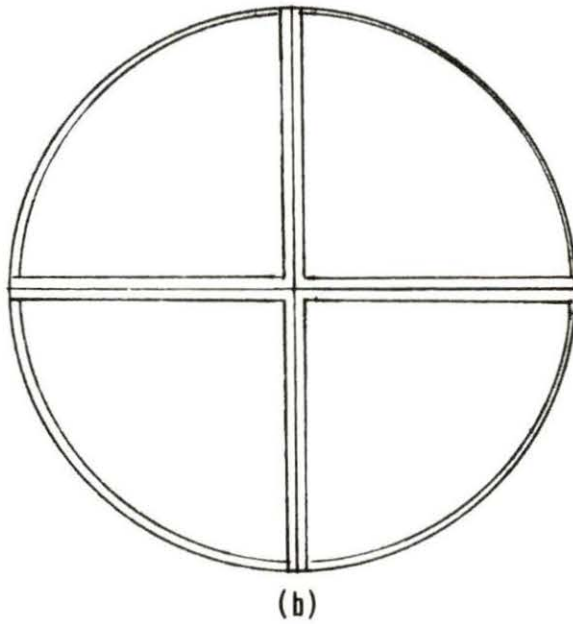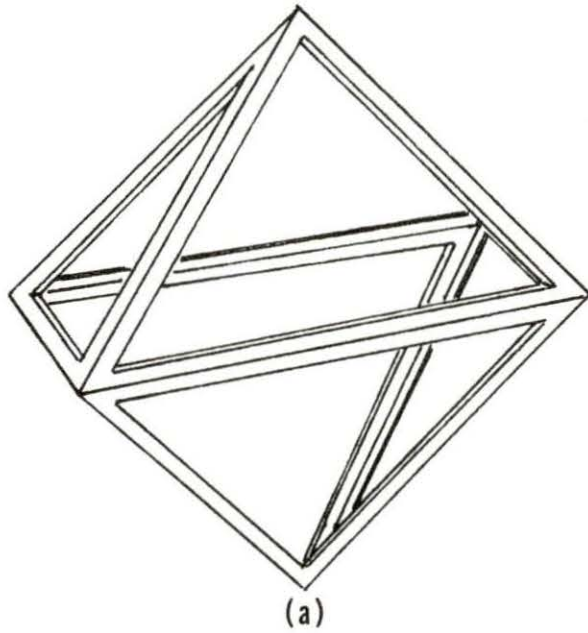
Fig. 7.1. Two new Osmac configurations
   (a) Osmac configuration using plane triangular coils
   (b) Osmac configuration using spherical triangular
       coils

across the center of the geometry. This hybrid Osmac trap, in combination with recommendation one, essentially functions as a stabilized mirror.

4. The OMIN code (Appendix B), should be modified to calculate the magnetic inductions of finite dimension coils. However accurate away from the loop, the filamentary conductor model has a singularity in the neighborhood of the filamentary conductor.

Graphical analysis of any of the above modifications to the current Osmac model would be greatly expedited by incorporating the OMIN code into a search routine to perform a point-by-point mapping of iso-$|\vec{B}|$ lines. The increased computation costs would more than offset the time spent for tedious graphical techniques currently used to produce iso-$|\vec{B}|$ plots.

LITERATURE CITED

1. Bishop, Amasa S. 1958. Project Sherwood, the U.S. program in controlled fusion. Addison Wesley Publishing Co., Reading, Mass.

2. Spalding, I. 1971. Cusp containment. Pages 79-123 in A. Simon and W. B. Thompson, eds. Advances in plasma physics. Interscience, New York, N.Y.

3. Chandrasekhar, S. 1960. Plasma physics. University of Chicago Press, Chicago, Ill.

4. Schmidt, J. 1966. Physics of high temperature plasmas. Academic Press, New York, N.Y.

5. Chiu, Y. C. 1973. Design of a magnetic well with tetrahedral symmetry. M.S. Thesis. Iowa State University, Ames, Iowa. 50 pp.

6. Valfells, Agust, et al. Feb. 8, 1977. US Patent 4007392.

7. Taylor, J. B. 1963. Some stable plasma equilibria in combined mirror-cusp fields. Physics of Fluids 6:1529-1537.

8. Berkowitz, J., K. O. Friedrichs, H. Goertzel, H. Grad, J. Killeen, and E. Rubin. 1958. Cusped geometries. Proc. Second U. N. Conference on the Peaceful Uses of Atomic Energy, Geneva 31:171-176.

9. Kitsunezaki, A., M. Tanimoto, and T. Sekiguchi. 1974. Cusp confinement of high-beta plasmas produced by a laser pulse from a freely-falling deuterium ice pellet. Physics of Fluids 17:1895-1902.

10. Hershkowitz, N., K. N. Leung, and T. Romesser. 1975. Plasma leakage through a low-β line cusp. Physical Review Letters 35:277-280.

11. Sadowski, M. 1967. Plasma containment with spherical multipole magnetic field. Physics Letters 25A:695-696.

12. Sadowski, M. 1970. Plasma confinement in a spherical multipole magnetic trap. Journal of Plasma Physics 4:1-12.

13. Owen, G. E. 1963. Introduction to electromagnetic
       theory. Allyn and Bacon, Inc., Boston, Mass.

ACKNOWLEDGMENTS

APPENDIX A: DERIVATION OF THE VECTOR

POTENTIAL (EQ. 4-10)

By the following algebraic manipulations the coefficients of the $\hat{i}$ and $\hat{j}$ unit vectors of Eq. 4-9 can be derived from the coefficients of the $\hat{i}$ and $\hat{j}$ unit vectors in Eq. 4-4. Since $\vec{A}_0(\xi = 0)$ can be generalized for any $\vec{A}_p$,

$$\frac{-a\,\sin\phi}{\sqrt{\rho^2 + a^2 + z^2 - 2a\rho\cos\phi}} = \frac{-a\,\sin\phi}{\sqrt{[(a+\rho)^2 + z^2] - 2a\rho(1-\cos\phi)}} \tag{A-1}$$

where $2a\rho$ has been added and subtracted in the denominator. Factoring $[(a+\rho)^2 + z^2]$ out of the denominator and using Eqs. 4-6 and 4-8, Eq. A-1 can be written

$$\frac{-a\,\sin\phi}{\sqrt{\rho^2 + a^2 + z^2 - 2a\rho\cos\phi}} = \frac{-a\,\sin\phi}{\sqrt{[(a+\rho)^2 + z^2][1-k^2\sin^2\alpha]}} \tag{A-2}$$

Again using Eq. 4-6

$$\frac{-a\,\sin\phi}{\sqrt{\rho^2 + a^2 + z^2 - 2a\rho\cos\phi}} = \frac{-k\sqrt{a/\rho}\sqrt{\sin^2\phi}}{2\sqrt{1 - k^2\sin^2\phi}} \tag{A-3}$$

$$= \frac{-k\sqrt{a/\rho}\sqrt{4\sin^2\alpha\cos^2\alpha}}{\sqrt{1 - k^2\sin^2\alpha}} \tag{A-4}$$

Finally,

$$\frac{-a\,\sin\phi}{\sqrt{\rho^2 + a^2 + z^2 - 2a\rho\cos\phi}} = \frac{-k\sqrt{a/\rho}\; 2\,\sin\alpha\,\cos\alpha}{\sqrt{1 - k^2\,\sin^2\alpha}} \qquad (A\text{-}5)$$

By a similar manipulation of the coefficients of $\hat{j}$ the result is Eq. 4-9,

$$\vec{A}_0 = \frac{\mu_0 Ik}{4\pi}\sqrt{\frac{a}{\rho}}\left[\hat{i}\int_{\frac{\pi}{2}}^{-\frac{\pi}{2}}\frac{2\sin\alpha\cos\alpha\,d\alpha}{\sqrt{1-k^2\sin^2\alpha}} - \hat{j}\int_{\frac{\pi}{2}}^{-\frac{\pi}{2}}\frac{(2\sin^2\alpha - 1)\,d\alpha}{1-k^2\sin^2\alpha}\right] \qquad (4\text{-}9)$$

To calculate the first integral let $x = \sin\alpha$, $dx = \cos\alpha\,d\alpha$.
Then,

$$\int_{\frac{\pi}{2}}^{-\frac{\pi}{2}}\frac{2\sin\alpha\cos\alpha\,d\alpha}{\sqrt{1 - k^2\sin^2\alpha}} = 2\cdot\int_{1}^{-1}\frac{x\,dx}{\sqrt{1-k^2x^2}} \qquad (A\text{-}6)$$

$$= \frac{1}{k^2}\left.\sqrt{1-k^2x^2}\,\right|_{1}^{-1}$$

$$= 0.$$

For the second integral,

$$-\int_{\frac{\pi}{2}}^{-\frac{\pi}{2}}\frac{(2\sin^2\alpha-1)\,d\alpha}{\sqrt{1-k^2\sin^2\alpha}} = 4\cdot\int_{0}^{\frac{\pi}{2}}\frac{\sin^2\alpha\,d\alpha}{\sqrt{1-k^2\sin^2\alpha}} - 2\cdot\int_{0}^{\frac{\pi}{2}}\frac{d\alpha}{\sqrt{1-k^2\sin^2\alpha}}$$

$$(A\text{-}7)$$

The second integral on the right hand side of Eq. A-7 is the complete elliptic integral of the first kind, K(k). By adding and subtracting 1 to the integrand of the first integral on the right hand side of Eq. A-7 we get,

$$
4 \cdot \int_0^{\frac{\pi}{2}} \frac{(1-1+k^2\sin^2\alpha)\,d\alpha}{k^2\sqrt{1-k^2\sin^2\alpha}} = \frac{4}{k^2} \cdot \left[\int_0^{\frac{\pi}{2}} \frac{d\alpha}{\sqrt{1-k^2\sin^2\alpha}} - \int_0^{\frac{\pi}{2}} \frac{(1-k^2\sin^2\alpha)\,d\alpha}{\sqrt{1-k^2\sin^2\alpha}} \right]
$$

$$(A-8)$$

The first integral on the RHS of Eq. A-8 is the complete elliptic integral of the first kind and the second integral on the RHS of Eq. A-8 is the complete elliptic integral of the second kind, E(k). Combining elliptic integrals, the coefficient of $\hat{j}$ reduces to,

$$
- \int_{\frac{\pi}{2}}^{-\frac{\pi}{2}} \frac{(2\sin^2\alpha-1)\,d\alpha}{\sqrt{1-k^2\sin^2\alpha}} = 2 \left[\left(\frac{2}{k^2} - 1\right) K(k) - \frac{2}{k^2} E(k) \right]. \qquad (A-9)
$$

Equation 4-9, in terms of complete elliptic integrals, can be written as

$$
\vec{A}_0 = \frac{\mu_0 I k}{2\pi} \sqrt{\frac{a}{\rho}} \left[\left(\frac{2}{k^2} - 1\right) K(k) - \frac{2}{k^2} E(k) \right] \hat{j}. \qquad (A-10)
$$

Factoring out a $2/k^2$ term, and generalizing for any angle ξ,

$$\vec{A}_p = \frac{\mu_0 I}{\pi k} \sqrt{\frac{a}{\rho}} \left[\left(1 - \frac{k^2}{2} \right) K(k) - E(k) \right] \hat{\phi} \ . \qquad \text{(A-11)}$$

APPENDIX B: THE OMIN CODE

The OMIN code has been developed to calculate the
magnetic induction at any point in the principal coordinate
system of Osmac geometry. OMIN is an accronym for Osmac
Magnetic INduction.

The OMIN code has been designed to compute the magnetic
induction along any radius of Osmac at a constant specified
interval. Required inputs are the ϕ and θ directions of the
radius in degrees, the radial interval length in centimeters,
and the initial and final points along the radius between
which the point-by-point magnetic induction is to be computed.

The OMIN code also has the capability of computing the
magnetic induction along a specified series of radii in planes
which contain either the z_0-axis (a P_1 plane) or the $z_0 = 0$
(P_2) plane. A particular P_1 plane is fixed by it ϕ angle.
Radii in that plane are separated by the constant θ increment
$\Delta\theta$. For the P_2 plane $\theta = 90°$ and radii are separated by the
constant ϕ increment $\Delta\phi$.

Also included as input are the loop current I(amps), the
loop radius R(cm), and an option for printing the vector
components of the total induction vector in rectangular
components.

OMIN input thus consists of two cards with the following
format:

```
(2F10.4,I5)CURRNT,RADIUS,JOPT

(9F8.5)PHI,DPHI,EPHI,THETA,DETHETA,ETHETA,RHO,DRHO,ERHO
```

```
CCCCCCCCCCCCCCCCCCCCCCCCCCCCCCCCCCCCCCCCCCCCCCCCCCCCCCCCCCCCCCCCCCCCCCC
C
C FUNCTION OF PROGRAM
C     OMIN COMPUTES THE MAGNETIC INDUCTION AT ANY POINT FOR THE OSMAC CURRENT
C     LOOP CONFIGURATION
C
CCCCCCCCCCCCCCCCCCCCCCCCCCCCCCCCCCCCCCCCCCCCCCCCCCCCCCCCCCCCCCCCCCCCCCCCC
C
CCCCCCCCCCCCCCCCCCCCCCCCCCCCCCCCCCCCCCCCCCCCCCCCCCCCCCCCCCCCCCCCCCCCCCCCC
C
C DEFINITION OF MPRGM AND SUBROUTINE LINE ARRAYS AND VARIABLES
C
CCCCCCCCCCCCCCCCCCCCCCCCCCCCCCCCCCCCCCCCCCCCCCCCCCCCCCCCCCCCCCCCCCCCCCCCC
C
CCCCCCCCCCCCCCC
C     ARRAYS    C
CCCCCCCCCCCCCCCC
C
C     ARRAY = TEN ELEMENT HOLDING ARRAY FOR TEN COLUMN FORMAT CF INDUCTION
C         MAGNITUDE (SEE 'TOTAL')
C     BTOTAL = THREE ELEMENT ARRAY CONTAINING COMPONENTS OF TOTAL INDUCTION
C         VECTOR
C     FIELD = 3 X 8 ARRAY WHICH CONTAINS THE COMPONENTS OF THE MAGNETIC INDUCTION
C         VECTOR FOR EACH LOOP-PAIR COORDINATE SYSTEM (COLUMNS 1,2,3,4) AND
C         THESE LOOP-PAIR COMPONENTS IN TERMS OF THE PRINCIPLE COORDINATE
C         SYSTEM (COLUMNS 5,6,7,8)
C     VECTOR = 3X5 ARRAY CONTAINING THE COORDINATES OF A POINT FOR EACH OF THE
C         FIVE COORDINATE SYSTEMS(PRINCIPLE + FOUR LOOP-PAIR SYSTEMS)
C     TRANSF = 3X3X4 ARRAY FOR TRANSFORMING POSITICN OR INDUCTION VECTORS
C         TO/FROM PRINCIPLE AND LOOP-PAIR SYSTEMS
CCCCCCCCCCCCCCCCCCC
C     VARIABLES    C
CCCCCCCCCCCCCCCCCCCC
C     CPHI = COS OF THE AZIMUTHAL ANGLE PHI IN SPHERICAL COORDINATES
C     CTHETA = COS OF THE POLAR ANGLE THETA IN SPHERICAL COORDINATES
C     CURRNT = FILAMENTARY LOOP CURRENT
```

```
C     DPHI = INCREMENTAL PHI ANGLE
C     DRHO = INCREMENTAL RADIAL ELEMENT IN SPHERICAL COORDINATES
C     DTHETA = INCREMENTAL THETA ANGLE
C     ERHO = TERMINAL LENGTH OF RADIUS IN SPHERICAL COORDINATES
C     EPHI = TERMINAL ANGLE IN PHI DIRECTION
C     ETHETA = TERMINAL ANGLE IN THETA DIRECTION
C     GTHETA = DUMMY VARIABLE, RETAINS INITIAL VALUE OF THETA FOR RECYCLE
C         AT THE END OF A DO LOOP
C     ICNTR = SPECIFIES INDEX FOR DO LOOP ON THETA ANGLE
C     INDEX = SPECIFIES INDEX FOR DO LOOP FOR POINT BY POINT CALCULATIONS ALONG
C         RHO
C     JOPT = OPTION TO PRINT COMPONENTS OF TOTAL POINT MAGNETIC INDUCTION
C         JOPT = 0, NO PRINT
C         JOPT = 1, PRINT
C     KCNTR = INDEX FOR DO LOOP ON PHI ANGLE
C     PHI = INITIAL AZIMUTHAL ANGLE OF RADIUS VECTOR IN SPHERICAL COORDINATES
C         WHICH IS THE POSITION VECTOR OF A POINT IN PRINCIPLE RECTANGULAR
C         COORDINATES
C     RADIUS = RADIUS OF FILAMENTARY CURRENT LOOP
C     RHO = RADIAL DISTANCE OF A POINT IN PRINCIPLE COORDINATES FROM ORIGIN AND
C         INITIAL POINT FOR INDUCTION CALCULATION ALONG A RADIUS
C     SPHI = SINE OF PHI
C     STHETA = SINE OF THETA
C     THETA = INITIAL POLAR ANGLE OF POSITION VECTOR IN SPHERICAL COORDINATES
C     TOTAL = MAGNITUDE OF THE TOTAL INDUCTION VECTOR AT A POINT IN THE
C         PRINCIPLE COORDINATE SYSTEM
C     XRHO = DUMMY VARIABLE TO RETAIN INITIAL VALUE OF RHO WHEN PASSING RHO
C         BETWEEN MPRGM AND SUBROUTINE LINE
C
CCCCCCCCCCCCCCCCCCCCCCCCCCCCCCCCCCCCCCCCCCCCCCCCCCCCCCCCCCCCCCCCCCCCCCCCCCCCC
C
C-----DIMENSION ARRAYS, SPECIFY COMMON DATA LOCATIONS
C
      DIMENSION ARRAY(10), BTOTAL(3), FIELD(3,8),VECTOR(3,5),TRANSF(4
     1,3,3)
      COMMON/STORE/BTOTAL,FIELD,TRANSF,VECTOR
      COMMON/A/ARRAY
```

```
      COMMON/INPUT/CURRNT,RADIUS,JOPT
      COMMON/T/TOTAL
      COMMON/R/RHO
      COMMON/PARAM/DRHO,ERHO,PHI,THETA
      COMMON/DEGREE/SPHI,CPHI,STHETA,CTHETA
C
C-----SPECIFY ELEMENTS CF TRANSF, SET VARIABLES TC ZERO
C
      DATA TRANSF/-.70711,-.70711,.70711,.70711,-.40825,-.40825,.40825,
     $.40825,.57735,.57735,-.57735,-.57735,.70711,-.70711,-.70711,.70711
     $,-.40825,.40825,.40825,-.40825,.57735,-.57735,-.57735,.57735,.0,.0
     $,.0,.0,.81650,-.81650,.81650,-.81650,.57735,-.57735,.57735,-.57735
     $/
      DATA ARRAY, BTOTAL, FIELD, VECTOR /52*0.0/
      DATA CURRNT ,RADIUS,TOTAL,RHO,DRHO,ERHO,PHI,DPHI,EPHI,THETA,
     1DTHETA,ETHETA,SPHI,CPHI,STHETA,CTHETA,JOPT/16*0.0,0/
      DATA ROTS,RADS,QUC/3*0.0/
      DATA KCNTR,ICNTR,INDEX/3*0/
C
C-----WRITE ELEMENTS CF TRANSF
C
      WRITE(6,605)
  605 FORMAT('0',40X,'**TRANSFORMATION MATRICES**')
      WRITE(6,606)
  606 FORMAT('0',9X,'P(0)-P(1)',18X,'P(0)-P(2)',17X,'P(0)-P(3)',17X,'P(0
     1)-P(4)')
      DO 35 J=1,3
      WRITE(6,607)((TRANSF(I,J,K),K=1,3),I=1,4)
  607 FORMAT(' ',4(2X,3F8.5))
   35 CONTINUE
C
C-----READ/WRITE CURRENT, RADIUS, JOPT
C
      READ(5,301)CURRNT,RADIUS,JOPT
  301 FORMAT(2F10.4,I5)
      WRITE(6,608)CURRNT,RADIUS,JOPT
```

```
  608 FORMAT('0','CURRENT =',F10.4,1X,'AMPS',5X,'RADIUS =',F10.4,1X,
     1'CM',5X,'JOFT',1X,I1)
C
C-----READ/WRITE PHI,DPHI,EPHI,THETA,DTHETA,ETHETA,RHO,DRHO,ERHO
C
      READ(5,77)PHI,DPHI,EPHI,THETA,DTHETA,ETHETA,RHO,DRHO,ERHO
   77 FORMAT(9F8.5)
      WRITE(6,177)
  177 FORMAT('0','PHI',7X,'DPHI',6X,'EPHI',6X,'THETA',5X,'DTHETA',4X
     1,'ETHETA',4X,'RHO',7X,'DRHO',6X,'ERHO')
      WRITE(6,178)PHI,DPHI,EPHI,THETA,DTHETA,ETHETA,RHO,DRHO,ERHO
  178 FORMAT(' ',9(F5.2,5X))
      IF(DPHI + DTHETA.NE.0.)GO TO 333
C
C-----IF DETHETA = DPHI = 0.0, COMPUTATION IS ALONG A LINE ONLY
C
      CALL LINE
      GO TO 713
  333 CONTINUE
      IF(DPHI.EQ.0.)GOTO 213
C
C-----IF DPHI ONLY IS EQUAL TO 0.0,COMPUTING IS IN ONE P(1) PLANE ONLY
C
      KCNTR = (EPHI-PHI)/DPHI + 1
      IF(DTHETA.EQ.0.) GOTO 214
C
C-----IF DTHETA ONLY IS EQUAL TO 0.0, COMPUTING IS IN THE P(2) PLANE OR A CONE
C-----IF BOTH DTHETA AND DPHI ARE NOT 0.0, COMPUTATION IS IN MORE THAN ONE P(1)
C           PLANE
      ICNTR = (ETHETA-THETA)/DTHETA + 1
      GTHETA = 0.0
      GTHETA=THETA
      PHI = PHI - DPHI
      DO 513 M = 1,KCNTR
      THETA=GTHETA
      PHI = PHI + DPHI
```

```
      WRITE(6,82)PHI
   82 FORMAT('0','PHI = ',F10.7)
      THETA = THETA-DTHETA
      DO 613 N=1,ICNTR
      THETA = THETA + DTHETA
      WRITE(6,73)THETA
   73 FORMAT(' ','THETA =',F5.2)
      CALL LINE
  613 CONTINUE
  513 CONTINUE
      GO TO 713
  213 CONTINUE
      ICNTR = (ETHETA-THETA)/DTHETA + 1
      THETA = THETA - DTHETA
      DO 313 M = 1,ICNTR
      THETA = THETA + DTHETA
      WRITE(6,72)THETA
   72 FORMAT(' ','THETA =',F5.2)
      CALL LINE
  313 CONTINUE
      GO TO 713
  214 PHI = PHI-DPHI
      DO 913 N = 1,KCNTR
      PHI = PHI + DPHI
      WRITE(6,82)PHI
      CALL LINE
  913 CONTINUE
  713 CONTINUE
      STOP
      END
```

```
C
C FUNCTION OF SUBROUTINE LINE
C       CONVERTS THE PHI AND THETA ANGLES TO RADIANS, COMPUTES THE SINE AND COSINE
C           OF THETA AND PHI, PASSES POINTS INTO SUBROUTINE BFIELD FOR INDUCTION
C           CALCULATION
        SUBROUTINE LINE
        COMMON/DEGREE/SPHI,CPHI,STHETA,CTHETA
        COMMON/R/RHO
        COMMON/T/TOTAL
        COMMON/A/ARRAY(10)
        COMMON/PARAM/DRHO,ERHO,PHI,THETA
        PHI = PHI*.01745329
        THETA = THETA*.01745329
        SPHI =SIN(PHI)
        CPHI = COS(PHI)
        STHETA = SIN(THETA)
        CTHETA = COS(THETA)
C
C------CONVERT THETA AND PHI TO DEGREES FOR PASSING BACK TO MPRGM
C
        PHI = PHI*57.29577951
        THETA = THETA*57.29577951
        XRHO = RHO
        N = 1
C
C------COMPUTE THE NUMBER OF POINTS ALONG RHO WHERE THE INDUCTION WILL BE
C         COMPUTED
C
        INDEX = (ERHO-RHO)/DRHO + 1
        RHO = RHO - DRHO
        DO 413 M = 1,INDEX
        RHO = RHO + DRHO
C
C------CALCULATE INDUCTION AT EACH POINT ALONG RHO AND PLACE MAGNITUDE INTO ARRAY
C
        CALL BFIELD
```

```
      ARRAY(N) = TOTAL
      N = N + 1
      IF(10-N)1,413,413
C
C-----WRITE ARRAY WHEN FULL
C
    1 WRITE(6,3)(ARRAY(I),I = 1,10)
    3 FORMAT(' ',10F10.3)
C
C-----RESET ARRAY TO ZERO
C
      DO 39 J = 1,10
      ARRAY(J) = 0.0
   39 CONTINUE
      N = 1
  413 CONTINUE
      IF(ARRAY(1).NE.0.)WRITE(6,3)(ARRAY(I),I=1,10)
      DO 97 J = 1,10
      ARRAY(J) = 0.0
   97 CONTINUE
      RHO = XRHO
      RETURN
      END
C FUNCTION OF THE SUBROUTINE BFIELD
C     COMPUTES THE MAGNETIC INDUCTION AT A POINT P(0) CONTRIBUTED BY EACH CURREN
C          LOOP AND SUMS THE CONTRIBUTIONS
C     DEFINITION OF SUBROUTINE BFIELD VARIABLES
C
C     NOTE: SINGLE ' REFERS TO CURRENT LOOP AXISYMMETRIC WITH THE POSITIVE Z
C          AXIS OF A LOOP-PAIR. DOUBLE '' REFERS TO CURRENT LOOP AXISYMMETRIC WITH
C          THE NEGATIVE Z AXIS OF A LOOP-PAIR
C     ASUBP = RADIAL POSITION OF P(N) IN A CYLINDER COORDINATE SYSTEM FOR EACH
C          COIL PAIR.
C     BEEPA = B'(N) IN THE RADIAL DIRECTION OF A POSITIVE CURRENT LOOP.
C     BEEPPA = B''(N) IN THE RADIAL DIRECTION OF A NEGATIVE CURRENT LOOP.
C     BEEPZ = B'(N) IN THE Z-DIRECTION OF A POSITIVE CURRENT LOOP.
```

```
C          BEEPPZ = B''(N) IN THE Z-DIRECTION OF A NEGATIVE CURRENT LOOP.
C          BEETA = BEEPA + BEEPPA
C          BEETX = B(N) IN THE X-DIRECTION
C          BEETY = B(N) IN THE Y-DIRECTION
C          BEETZ = BEEPZ + BEEPPZ
C          COEFF = (0.001*CURRNT)/(SQRT(RADIUS)).
C          DENOM = ASUBP**1.5
C          EKP = ELIPTIC INTEGRAL OF THE SECOND KIND OF K'.
C          EKPP = ELIPTIC INTEGRAL OF THE SECOND KIND OF K''.
C          EPA = THE VALUE OF B(N), N = 1,2,3,4 IN THE RADIAL DIRECTION OF A
C             CYLINDRICAL SYSTEM FOR A POSITIVE LOOP.
C          EPPA = THE VALUE OF B(N), N = 1,2,3,4 IN THE RADIAL DIRECTION OF A
C             CYLINDRICAL SYSTEM FOR A NEGATIVE CURRENT LOOP.
C          EPPZED = THE VALUE OF B(N), N = 1,2,3,4 IN THE Z-DIRECTION OF A CYL. COOR.
C             SYSTEM FOR A NEGATIVE CURRENT LOOP.
C          EPZED = THE VALUE OF B(N), N = 1,2,3,4 IN THE Z-DIRECTION OF CYL. COOR.
C             SYSTEM FOR A POSITIVE CURRENT LOOP.
C          FACTP = COEFFICIENT OF THE SUM OF ELIPTIC INTEGRAL TERMS OF A POSITIVE
C             LOOP.
C          FACTPP = COEFFICIENT OF THE SUM OF ELIPTIC INTEGRAL TERMS OF A NEGATIVE
C             CURRENT LOOP.
C          KKP = ELIPTIC INTEGRAL OF THE FIRST KIND OF MODULUS K'.
C          KKPP = ELIPTIC INTEGRAL OF THE FIRST KIND OF K''.
C          SMODP = SQRT(XMODP).
C          SMODPP = SQRT(XMODPP).
C          THETA = ANGLE OF ASUBP WITH RESPECT TO X(N) AXIS
C          XMODP = MODULUS K'**2 OF A POSITIVE LOOP.
C          XMODPP = MODULUS K'**2 OF A NEGATIVE LOOP
C          XSUBP = X-VALUE OF P(N) IN N = 1,2,3,4 COORDINATE SYSTEM.
C          YSUBP = Y-VALUE OF P(N) IN N = 1,2,3,4 COORDINATE SYSTEM
C          ZETAP = Z', THE DISTANCE OF P(N) FROM THE POSITIVE CURRENT LOOP
C             AXIALLY SYMMETRIC WITH THE +Z(N) AXIS, N = 1,2,3,4.
C          ZETAPP = Z'', THE DISTANCE OF P(N) FROM NEGATIVE CURRENT LOOP AXIALLY
C             SYMMETRIC WITH THE -Z(N) AXIS, N = 1,2,3,4
C
C
```

```
      SUBROUTINE BFIELD
      COMMON/DEGREE/SPHI,CPHI,STHETA,CTHETA
      COMMON/STORE/BTOTAL(3),FIELD(3,8),TRANSF(4,3,3),VECTOR(3,5)
      COMMON/T/TOTAL
      COMMON/R/RHC
      COMMON/INPUT/CURRNT,RADIUS,JOPT
      REAL KKP,KKPP
C
C-----CONVERT PRINCIPLE SPHERICAL COORDINATES TO PRINCIPLE RECTANGULAR
C        COORDINATES
C
      VECTOR(1,1)=RHO*STHETA*CPHI
      VECTOR(2,1)=RHO*SPHI*STHETA
      VECTOR(3,1) = RHO*CTHETA
C
C-----COMPUTE THE COORDINATES OF P(O) FOR EACH LOOP-PAIR COORDINATE SYSTEM
C
      DO 70 LEVEL=1,4
      DO 80 IROW=1,3
      SUM=0.0
      KCOL=0
      DO 90 JCOL=1,3
      PROD = VECTOR(JCOL,1)*TRANSF(LEVEL,IROW,JCOL)
      SUM = SUM + PROD
   90 CONTINUE
      KCOL = LEVEL + 1
      VECTOR(IROW,KCOL) = SUM
   80 CONTINUE
   70 CONTINUE
      DO 11 K=2,5
      L=1
      M=2
      N=3
C
C-----COMPUTE THE COORDINATES OF P(O) FOR EACH LOOP OF THE LOOP-PAIR WITH
C        RESPECT TO THE LOOP-PAIR COORDINATE SYSTEM
```

```
      ZETAP = VECTOR(N,K) - (.70711*RADIUS)
      ZETAPP = VECTOR(N,K) + (.70711*RADIUS)
      XSUBP = VECTOR(L,K)
      YSUBP = VECTOR(M,K)
      ASUBP = SQRT(XSUBP*XSUBP + YSUBP*YSUBP)
      IF(ASUBP.LE.1.0E-02)ASUBP=0.0
C
C-----CALCULATE THE MODULUS K OF K(K) AND E(K) FOR EACH LOOP OF THE LOOP-PAIR
C
      XMODP = (4.0*RADIUS*ASUBP)/((ASUBP + RADIUS)**2.0 + ZETAP*ZETAP)
      XMODPP=(4.0*RADIUS*ASUBP)/((ASUBP+RADIUS)**2.0+ZETAPP*ZETAPP)
      SMODP = SQRT(XMODP)
      SMODPP = SQRT(XMODPP)
      AK = SMODP
      A = 1.0
      B = 1.0
C
C-----CALL CEL(2) TO COMPUTE THE VALUES OF K(K) AND E(K) FOR EACH LOOP
C
      CALL CEL2(RES,AK,A,B,IER)
      KKP = RES
      AK = SMODPP
      B = 1.0
      CALL CEL2(RES,AK,A,B,IER)
      KKPP = RES
      AK = SMODP
      B = 1.0 - (AK*AK)
      CALL CEL2(RES,AK, A,B,IER)
      EKP = RES
      AK = SMODPP
      B = 1.0 - (AK*AK)
      CALL CEL2(RES,AK,A,B,IER)
      EKPP = RES
      COEFF = (0.1*CURRNT)/(SQRT(RADIUS))
      DENOM = ASUBP**1.5
```

```
       IF(DENOM)81,81,85
C
C-----IF ASUBP = 0.0 COMPUTE INDUCTION ALONG Z-AXIS ONLY FOR EACH LOOP AND ADD
C
    81 COEFF = (.6283*CURRNT*RADIUS*RADIUS)
       BEEPZ = COEFF/((RADIUS*RADIUS + ZETAP*ZETAP)**1.5)
       BEEPPZ = COEFF/((RADIUS*RADIUS + ZETAPP*ZETAPP)**1.5)
       BEETZ = BEEPZ + BEEPPZ
       BEETX = 0.0
       BEETY = 0.0
       L = K - 1
       J = 1
       GO TO 87
    85 CONTINUE
C
C-----COMPUTE INDUCTION ALONG LOOP-PAIR Z-AXIS AND ASUBP AXIS IN THE X-Y PLANE
C
       FACTP = SMODP/DENOM
       FACTPP = SMODPP/DENOM
       EPA = -ZETAP*(KKP-((1.0-XMODP/2.0)*EKP)/(1.0-XMODP))
       EPPA = -ZETAPP*(KKPP-((1.0-XMODPP/2.0)*EKPP)/(1.0-XMODPP))
       EPZED = ASUBP*(KKP+(((RADIUS+ASUBP)*XMODP)/(2.0*ASUBP)-1.0)*EKP
      1/(1.0-XMODP))
       EPPZED = ASUBP*(KKPP+(((RADIUS+ASUBP)*XMODPP)/(2.0*ASUBP)-1.0)*
      1EKPP/(1.0-XMODPP))
       L=K-1
       J=1
       BEETA = COEFF*(FACTP*EPA + FACTPP*EPPA)
       BEETZ = COEFF*(FACTP*EPZED + FACTPP*EPPZED)
       IF(ABS(XSUBP).GT.0.001)GO TO 76
    75 BEETX = 0.0
       BEETY = BEETA
       GO TO 87
    76 CONTINUE
C
C-----COMPUTE THE X AND Y COMPONENTS OF INDUCTION IN RECTANGULAR COORDINATES
```

```
C
      IF(XSUBP.LT.0.)GOTO 5
      IF(YSUEP.GE.0.) GOTO7
      THETA = 6.283185308 +ATAN(YSUBP/XSUBP)
      GOTO 8
    7 THETA = ATAN(YSUBP/XSUBP)
      GOTO 8
    5 IF(YSUBP.LE.0.)GOTO 6
      THETA = 3.141592654 + ATAN(YSUBP/XSUBP)
      GOTO 8
    6 THETA = 3.141592654+ATAN(YSUBP/XSUBP)
    8 CONTINUE
      BEETX = BEETA*COS(THETA)
      BEETY = BEETA*SIN(THETA)
   87 CONTINUE
      FIELD(J,L) = BEETX
      J = J+1
      FIELD(J,L) = BEETY
      J = J+1
      FIELD(J,L) = BEETZ
   11 CONTINUE
C
C-----TRANSFORM THE FOUR LOOP-PAIR INDUCTION COMPONENTS INTO THE CORRESPONDING
C         PRINCIPLE COMPONENTS AND ADD.
C
      DO 15 LEVEL = 1,4
      DO 16 JCOL = 1,3
      SUM = 0.0
      DO 17 IROW = 1,3
      PROD = FIELD(IROW,LEVEL)*TRANSF(LEVEL,IROW,JCOL)
      SUM = SUM+PROD
   17 CONTINUE
      FIELD(JCOL,LEVEL + 4) = SUM
   16 CONTINUE
   15 CONTINUE
      DO 55 I = 1,3
      BTOTAL(I) = 0.0
   55 CONTINUE
```

```
      DO 31 I = 1,3
      DO 32 J=5,8
      BTOTAL(I) = BTOTAL(I) + FIELD(I,J)
   32 CONTINUE
   31 CONTINUE
      IF(JOPT.EQ.0)GOTO 4120
      WRITE(6,25)(BTOTAL(I),I = 1,3)
   25 FORMAT(' ',3F10.3)
 4120 CONTINUE
C
C-----COMPUTE THE MAGNITUDE OF THE TOTAL INDUCTION VECTOR
C
      TOTAL = 0.0
      DO 33 I = 1,3
      TOTAL = TOTAL + BTOTAL(I)*BTOTAL(I)
   33 CONTINUE
      TOTAL = SQRT(TOTAL)
      RETURN
      END
```